An Evaluation of Low-Order Finite Elements

by

Ramon Pereira da Silva

Submitted to the Department of Mechanical Engineering
in partial fulfillment of the requirements for the degree of

Master of Science

at the

MASSACHUSETTS INSTITUTE OF TECHNOLOGY

June 1999

Author .....
Department of Mechanical Engineering
April 12, 1999

Certified by .....
Klaus-Jürgen Bathe
Professor of Mechanical Engineering
Thesis Supervisor

Accepted by .....
Ain Ants Sonin
Chairman, Graduate Committee

An Evaluation of Low-Order Finite Elements

by

Ramon Pereira da Silva

Submitted to the Department of Mechanical Engineering
on April 12, 1999, in partial fulfillment of the
requirements for the degree of
Master of Science

Abstract

Due to their computational efficiency and generality, low-order finite elements are ideally used in engineering practice. However, standard displacement-based finite elements fail in the analysis of problems when near incompressible elasticity or bending-dominated behaviors are encountered. Various mixed interpolation procedures have been proposed and are extensively used to solve such problems. The purpose of this research is to survey and evaluate successful attempts in formulating reliable low-order mixed-interpolated finite elements. Surprisingly, most of the elements proposed in the literature have not yet been subjected to rigorous mathematical analysis. In particular, the authors did not evaluate whether the inf-sup condition is satisfied.

Thesis Supervisor: Klaus-Jürgen Bathe
Title: Professor of Mechanical Engineering

Acknowledgments

I would like to express my deepest gratitude to my supervisor, Prof. Klaus-Jürgen Bathe, for his encouragement and unfailing support. His great enthusiasm as a teacher is inspiring, and it is my pleasure to acknowledge his strong commitment in teaching and research at M.I.T.

I am grateful to M.I.T. for its hospitality and unique educational experience. In particular, I am grateful to Dawn Metcalf, Dr. Kristine Girard and Richard Goldhammer for their continued support and encouragement. I am also thankful to my colleagues at the Finite Element Research Group, Alex Iosilevich, Cora Martinez, Daniel Pantuso, Dena Hendriana, Jean-François Hiller, Sandra Rugonyis, Shingo Okamoto and Suvranu De.

My deepest appreciation also goes to my friends, Mrs. Emma and Abel Sanchez, Mrs. Liliany and Thomas Novacek, Ms. Melissa Araújo, and Mrs. Sônia and Hugo Bicalho, who made my staying at M.I.T. an enjoyable experience. My special thanks is due to Marco Meggiolaro, whose friendship I am delighted to acknowledge.

I am thankful to ADINA R&D, Inc. for allowing me to use their proprietary software ADINA{-IN,-F,-T,-PLOT} during the course of this work.

This work was partially supported by CAPES (the Brazilian Ministry of Education Funding Agency) and by UFMG (the Federal University of Minas Gerais), which is gratefully acknowledged. In particular, I am also thankful to my colleagues at the Structural Engineering Department.

My utmost gratitude is due to my wife, Jacira, whose love and encouragement constituted priceless support.

Contents

List of Figures

List of Tables

Chapter 1

Introduction

The pure displacement-based finite element method is widely used in practical engineering analysis. However, it is well known that displacement-based finite elements do not perform well in the analysis of certain problems, such as in the analysis of plates/shells and in near incompressible elasticity, exhibiting a too stiff response characterized in the literature as *locking* [1].

Shear locking occurs due to the inability of the discrete numerical model to properly represent a zero shear strain state for pure bending problems; hence, adding an erroneous shear strain energy contribution to the overall analysis. *Membrane locking* appears when artificial membrane strains are generated. These phenomena typically occur in beam and thin plate/shell analysis when the thickness of the element approaches zero. In near incompressible media analysis *volumetric locking* occurs due to the fact that the discrete numerical model does not have a sufficiently rich displacement field that satisfies the zero volumetric strains as the Poisson's ratio ν approaches the limit 1/2.

To overcome such (numerical) difficulties various techniques have been proposed. The main idea is to interpolate the strain and stress fields in addition to the displacement field, giving rise to the so called *mixed* methods.

The common basis of all mixed methods proposed in the literature is the general functional of Hu-Washizu [1], in which displacements, stresses and strains are used as independent variables (*mixed* fields). The finite element interpolations of these fields

can be chosen independently of each other. From the Hu-Washizu functional we can derive the Hellinger-Reissner (H-R) functional, in which case the displacements and stresses are the variables. Based on the H-R functional, Pian and Sumihara [2] developed a 4-node quadrilateral element, which has been reported in the literature to exhibit good convergence. See [3] and references therein.

In another approach, elements are derived using the Hu-Washizu functional, with displacement and strain fields as independent variables. The stresses are evaluated from the stress-strain material constitutive law. This class of mixed methods has been given considerable attention due to its intrinsic strain-driven nature, i.e., fitting effortless into the existing numerical algorithms used in nonlinear analysis. Some representative variants within this class of mixed methods are briefly summarized in the following:

The method of incompatible modes: in addition to the usual displacement interpolation functions, Wilson *et al* [4] proposed the use of incompatible displacement modes attempting to improve the predictive capability of the classical 4-node isoparametric element for plane stress/strain analysis. However, this element does not satisfy the patch test, limiting its application to meshes of parallelogram-type elements. Further work by Taylor *et al* [5] improved the performance of Wilson's element for distorted meshes and offered an alternative formulation for the element to satisfy the patch test.

The method of assumed strains: in the classical displacement-based finite element method the strains are derived from kinematic relations of the interpolated displacement field. A closer look at Wilson's element leads one to think of the incompatible displacements to make an additional contribution to the strain (displacement-based) field. The incompatible displacements pertain only to the element considered and are statically condensed out at the element level. Thus, one might be able to identify a "reasonable" correction or enhancement to the (displacement interpolated) strain field, provided this alternative element satisfies the minimum conditions to assure the consistency and stability of the numerical solution. Specifically we need that the element (*i.*) should be able to represent a constant strain state (the patch test), (*ii.*)

displays all natural rigid body mode displacements and, (*iii.*) does not contain any spurious energy modes (equivalent to say that the stiffness matrix contains no more zero eigenvalues than those related to the element's rigid body displacements).

Among the different options for designing an *enhanced strain* mixed-type element, the Mixed Interpolation of Tensorial Components (MITC) and the Enhanced Assumed Strain (EAS) are well established schemes researched and used in practice.

In the MITC scheme, a well-chosen interpolated strain field is tied to the interpolated displacement field at certain sampling points; thus, no additional modes are included in the analysis. The successful developments of Bathe and Dvorkin [6] in the context of plate/shell analysis have coined the concept of **M***ixed* **I***nterpolation of* **T***ensorial* **C***omponents* (MITC) in the finite element literature. Some examples of the successful use of the MITC scheme for linear and nonlinear stress analysis are described in [7, 8].

Simo and Rifai [9] have proposed a general variational-based framework for developing *E*nhanced *A*ssumed *S*train type elements. Starting from a three-field variational formulation, a rationale is proposed for designing mixed interpolated elements and at the same time satisfying the patch test. From this development, various new mixed finite elements for a broad range of analysis were proposed in the literature [10, 11].

In a related approach combinations of the above schemes are used. In the particular case of (almost) incompressible elasticity analysis, the pressure field (related to the volumetric strains) is interpolated separately, and the deviatoric strain field is calculated from the interpolated displacement field. If the pressure field is interpolated at the element level, termed u/p formulation, a discontinuous pressure field between elements is obtained [1]. In contrast to the u/p formulation, the u/p-c formulation renders a continuous pressure distribution over the element's boundaries, in which case the pressure is an additional nodal variable included in the analysis. Pantuso and Bathe [12] have proposed a mixed interpolated 4-node quadrilateral finite element for solid and fluid analysis using the u/p-c formulation and including an enhanced strain field. The element does not lock when either (almost) incompressible conditions or bending dominated problems are considered and passes the numerical

inf-sup test [13].

Due to their computational efficiency, generality and simple geometry, low-order finite elements exhibiting a locking-free response are ideal for practical engineering analysis. Nevertheless, all developments cited above focused on improving 4-node quadrilateral and 8-node hexaedron type of elements. Yet, an enhanced low-order 3-node triangular element (and corresponding 4-node tetrahedron for 3D analysis) is very desirable. Triangular elements are useful in modeling complex geometries, in which case quadrilateral elements are necessarily distorted, consequently deteriorating the element's performance.

In view of the above considerations and foreseeing the development of an improved 3-node triangular (and its 3D 4-node counterpart) finite element for solid analysis, the purpose of this work is to survey and evaluate successful attempts to develop low-order elements.

To guide this work, we have established some criteria attempting to reach our goal to have a reliable element, i.e, the element should, ideally, satisfy all the conditions below [6]:

- be continuum mechanics based
- satisfy the patch test
- be invariant and insensitive to geometric distortions
- have a minimum of stress/strain parameters
- provide accurate displacement and stress calculations irrespective of material conditions
- use full numerical integration
- use no artificial parameters
- satisfy the inf-sup condition (locking-free response and no spurious zero energy modes)

- work well in small and large strain conditions

Hence, we shall concentrate on formulations that can be cast into this framework.

The thesis outline is as follows. In Chapter 2 we introduce the notation used throughout the text and review the displacement and mixed finite element formulations. With these theoretical tools at hand, in Chapter 3 we summarize the developments published in the literature. In Chapter 4 we then compare the performance of finite elements in the solution of well known benchmark problems in linear static analysis. Finally, in Chapter 5 we close the presentation by mentioning general conditions to assure stability and convergence of mixed interpolation procedures.

Chapter 2

Formulation of the Finite Element Method: Review

2.1 Preliminary Remarks

Let $\mathcal{B}$ denote a solid body with volume Ω and surface area Γ with $\Omega \cap \Gamma = \varnothing$ such that $\overline{\Omega} = \Omega \cup \Gamma$ is a closed domain in $\mathbb{R}^3$. Adopting the Cartesian coordinate system as our (inertial) reference frame (X_1, X_2, X_3), the physical location of any point $\overline{\Omega} \subset \mathbb{R}^3$ is given by the components $\{x_1, x_2, x_3\}$ of the vector $\mathbf{x}$

$$\mathbf{x} = x_1\mathbf{e}_1 + x_2\mathbf{e}_2 + x_3\mathbf{e}_3 = x_i\mathbf{e}_i \tag{2.1}$$

where $\mathbf{e}_i$ is the i^{th} unit base vector of the rectangular Cartesian coordinate system. In Eq. (2.1) the summation convention over i $(i = 1, 2, 3)$ is implied[1].

Consider now the analysis of a solid body. We denote by Γ_u that part of Γ which contains the prescribed displacements $\mathbf{u}_p$ applied on Γ, and by Γ_f that part of Γ to which surface forces $\mathbf{f}^S$ and concentrated forces $\mathbf{f}_k^C$ (at a generic point k) are applied. The body is also subjected to body forces $\mathbf{f}^B$ on Ω.

[1]We also use comma to denote differentiation.

The general governing differential equations of this problem are given by [14]

$$\tau_{ij,j} + f_i^B = 0 \qquad \text{on } \Omega \tag{2.2}$$

$$\tau_{ij} n_j = f_i^S \qquad \text{on } \Gamma_f \tag{2.3}$$

$$u_i|_{\Gamma_u} = u_{p(i)} \qquad \text{on } \Gamma_u \tag{2.4}$$

where τ_{ij} are the components of the stress tensor $\boldsymbol{\tau}$, n_j is the j^{th} component of the outward unit normal vector to the surface Γ. The above equations form a "boundary value problem", and (2.2) is a statement of equilibrium at any point $\mathbf{x} \in \Omega$, whereas equations (2.3) and (2.4) are, respectively, the force (or *natural*) boundary conditions on Γ_f, and displacement (or *essential*) boundary conditions on Γ_u. To perform the analysis, it is necessary to supplement Eqs. (2.2–2.4) with assumptions on the material properties, stress-strain relationships, and kinematic conditions, such that all three fundamental requirements of mechanics are fulfilled[2]. We will restrict our attention to general linear elastic continuum problems, by assuming the following:

- the material properties do not depend on the stress state;
- *quasi*-static loading conditions apply;
- the displacements are infinitesimally small; thus, the unloaded configuration of the body is used to solve for the displacements and corresponding strains

Endowed with these assumptions, we have a constant stress-strain matrix $\mathbf{C}$ and use the following relations:

$$\tau_{ij} = C_{ijrs}\epsilon_{rs} \tag{2.5}$$

$$\epsilon_{ij} = \tfrac{1}{2}\left(u_{i,j} + u_{j,i}\right) \tag{2.6}$$

where ϵ_{ij} are the components of the small strain tensor $\boldsymbol{\epsilon}$ measured in the rectangular Cartesian coordinate system [15].

[2]Namely, (*i.*) equilibrium conditions; (*ii.*) compatibility; and (*iii.*) stress-strain law.

2.2 Principle of Virtual Work

An equivalent and general statement of equilibrium of our solid body is given by the "*principle of virtual work*" (2.7). In words, it requires that, for any admissible *virtual displacement* $\overline{\mathbf{u}}$ (and corresponding *virtual strains* $\overline{\boldsymbol{\epsilon}}$) imposed on a body at equilibrium,

"the internal virtual work equals the external virtual work."

By admissible virtual displacement an independent "imaginary" continuous displacement field is meant, which is zero at and corresponding to the actually prescribed displacements. The principle is expressed in the following equation:

$$\int_{\Omega} \overline{\boldsymbol{\epsilon}}^T \boldsymbol{\tau}\, d\Omega = \int_{\Omega} \overline{\mathbf{u}}^T \mathbf{f}^B\, d\Omega + \int_{\Gamma_f} \overline{\mathbf{u}}^{\Gamma_f^T} \mathbf{f}^S\, d\Gamma + \sum_k \overline{\mathbf{u}}_k^T \mathbf{f}_k^C \tag{2.7}$$

Observe that we use vector notation in Eq. (2.7). We also note that the small strain tensor can be thought of as obtained by the application of a linear differential operator $\boldsymbol{\partial}_\epsilon$ on the displacement field $\mathbf{u}$. Thus,

$$\boldsymbol{\epsilon} = \boldsymbol{\partial}_\epsilon \mathbf{u} \tag{2.8}$$

Writing Eq. (2.8) in vector notation gives:

$$\boldsymbol{\epsilon}(x_1, x_2, x_3) = \begin{bmatrix} \epsilon_{11} \\ \epsilon_{22} \\ \epsilon_{33} \\ 2\epsilon_{12} \\ 2\epsilon_{23} \\ 2\epsilon_{31} \end{bmatrix} = \begin{bmatrix} \frac{\partial}{\partial x_1} & 0 & 0 \\ 0 & \frac{\partial}{\partial x_2} & 0 \\ 0 & 0 & \frac{\partial}{\partial x_3} \\ \frac{\partial}{\partial x_2} & \frac{\partial}{\partial x_1} & 0 \\ 0 & \frac{\partial}{\partial x_3} & \frac{\partial}{\partial x_2} \\ \frac{\partial}{\partial x_3} & 0 & \frac{\partial}{\partial x_1} \end{bmatrix} \begin{bmatrix} u_1(x_1, x_2, x_3) \\ u_2(x_1, x_2, x_3) \\ u_3(x_1, x_2, x_3) \end{bmatrix} \tag{2.9}$$

Furthermore, since the virtual displacement is arbitrary, we can replace $\overline{u}_i$ in Eq. (2.7) by an arbitrary continuous function $v_i|_{\Gamma_u} = 0$. Then, for the specific case of linear elasticity Eq. (2.7) can be rewritten (in vector notation) as

$$\int_{\Omega} \overline{\boldsymbol{\epsilon}}^T \mathbf{C}\, \boldsymbol{\epsilon}\, d\Omega = \int_{\Omega} \mathbf{v}^T \mathbf{f}^B\, d\Omega + \int_{\Gamma_f} \mathbf{v}^{\Gamma_f^T} \mathbf{f}^S\, d\Gamma \tag{2.10}$$

where we have used the fact that $\boldsymbol{\tau} = \mathbf{C}\boldsymbol{\epsilon}$ and that all surface loads are contained in $\mathbf{f}^S = \{\mathbf{f}^S, \mathbf{f}^C\}$.

2.3 Displacement-Based Finite Element

Clearly, a closed-form solution of the above general boundary value problem is only possible for simple applications. Thus, in practical engineering situations, approximated solutions (of a well defined and carefully chosen mathematical model) are obtained by using classical approximation techniques such as the weighted residual methods, the finite difference method, or the Ritz method. The common basis of these techniques is that the solution u of a general boundary value problem

$$A(u) = f \qquad \text{on } \Omega \tag{2.11}$$

$$B(u)_i = g_i, \qquad \text{on } \Gamma \quad i = 1, 2, \ldots, n \tag{2.12}$$

is approximated in the form

$$u \approx \hat{u} = \sum_{j=1}^{p} \hat{u}_j \psi_j \tag{2.13}$$

$$R = A(\hat{u}) - f \tag{2.14}$$

where the ψ_j are assumed functions satisfying Eqs. (2.12) and the $\hat{u}_j$ are calculated such that the residual R in (2.14) is minimized. Therefore, using different criteria for choosing a particular set of functions $\boldsymbol{\psi}^h = \{\psi_1, \ldots, \psi_p\}$ as well as to evaluate the respective unknowns $\hat{\mathbf{u}}^h = \{\hat{u}_1, \ldots, \hat{u}_p\}$, result in different approximation techniques. However, a detailed discussion about this subject is lengthy and beyond our purpose. See for instance [1, 16].

In the finite element method (FEM) the displacement field $\mathbf{u}$ is approximated using a form similar to (2.13), and the principle of virtual work (2.7) is the criterion used to obtain the unknowns $\hat{\mathbf{u}}_j$. The essence of the FEM is that the body is idealized as a collection of n_e non-overlapping discrete finite elements Ω_e which are connected at nodal points lying on the element boundaries[3]. The great advantage of this approach is that, as opposed to using "global" (*trial*) functions $\psi_j \in \Omega$ as is the case of (2.13), the FEM uses a set of (*trial*) functions $\mathbf{h}_e = \{h_1(\Omega_e), \ldots, h_q(\Omega_e)\}$, which are *polynomials* specified at each node and correspond to the nodal unknowns

[3]Note that we may have nodal point(s) defined inside of each element.

in the finite element Ω_e. In our specific case, the multipliers $\hat{\mathbf{u}}_j$ are the unknown (global) nodal displacements, which are calculated by invoking the principle of the virtual work (PVW).

Note that the virtual displacements can be thought of as a set of *test* functions which, along with the PVW form the basis of the finite element approximation.

2.4 Properties of the FEM

In this section we assume that the prescribed displacements are zero. In order to understand some important properties of the FEM, it is expedient to adopt a compact notation. We rewrite Eq. (2.10) in the form $\mathcal{A}(\mathbf{u},\mathbf{v}) = \mathcal{F}(\mathbf{v})$ such that

$$\mathcal{A}(\mathbf{u},\mathbf{v}) = \int_\Omega (\boldsymbol{\partial}_\epsilon \mathbf{v})^T \, \mathbf{C} \, (\boldsymbol{\partial}_\epsilon \mathbf{u}) \, d\Omega \tag{2.15}$$

$$\mathcal{F}(\mathbf{v}) = \int_\Omega \mathbf{v}^T \mathbf{f}^B \, d\Omega + \int_{\Gamma_f} \mathbf{v}^{\Gamma_f^T} \mathbf{f}^S \, d\Gamma \tag{2.16}$$

Note that, since $\mathbf{C}$ is a symmetric tensor,

$$\mathcal{A}(\mathbf{u},\mathbf{v}) = \mathcal{A}(\mathbf{v},\mathbf{u}); \qquad \mathcal{A}(\mathbf{u},\mathbf{u}) > 0 \quad \text{if } \mathbf{u} \neq \mathbf{0}$$

Thus, Eq. (2.15) gives a measure of the internal energy of our elasticity problem. Hence, if we had chosen $\mathbf{v} = \mathbf{u}$, we would have obtained $\mathcal{A}(\mathbf{u},\mathbf{u}) = 2\,\mathcal{U}(\mathbf{u})$. We also note that although $\mathbf{v}$ is an arbitrary function with the constraint that $\mathbf{v}|_{\Gamma_u} = \mathbf{0}$, our elasticity problem requires that $\mathbf{v}$ and $\boldsymbol{\partial}_\epsilon \mathbf{v}$ be continuous in Ω *and*, since we are looking for solutions resulting in finite strain energy, we need to require that $\mathbf{v}$ and $\boldsymbol{\partial}_\epsilon \mathbf{v}$ be square-integrable, i.e., be members of $L^2(\Omega)$, which is defined as:

$$L^2(\Omega) = \left\{ \mathbf{w} \mid \mathbf{w} : \Omega \subset \mathbb{R}^3 \text{ and } \int_\Omega \sum_{i=1}^{3} (w_i)^2 \, d\Omega \equiv \|\mathbf{w}\|^2_{L^2(\Omega)} < +\infty \right\} \tag{2.17}$$

where $\|\cdot\|_{L^2}$ is the 2-norm defined in the space $L^2(\Omega)$.

With these observations in mind, we can proceed in defining the space V in which the exact solution $\mathbf{u}$ lies[4], namely:

$$V = \left\{ \mathbf{v} \mid (v_i, v_{i,j}) \in L^2(\Omega); \;\; v_i|_{\Gamma_u} = 0; \; i,j = 1,2,3 \right\} \tag{2.18}$$

[4]Note that, since we require that both v_i and its first general derivatives $(v_{i,j})$ be members of

To complete the definition of V it is necessary to specify a norm. Recalling that we are looking for solutions which correspond to finite strain energy and based on the fact that $\mathcal{A}(\mathbf{v},\mathbf{v})$ is itself a inner-product in V, we define the *energy norm*:

$$\|\mathbf{v}\|_E = \sqrt{\mathcal{A}(\mathbf{v},\mathbf{v})} \tag{2.19}$$

and we can regard V as a *normed linear vector space* [18]. Thus, our general elasticity problem reads [1]:

$$\text{Find} \quad \mathbf{u} \in V \quad \text{such that} \quad \mathcal{A}(\mathbf{u},\mathbf{v}) = \mathcal{F}(\mathbf{v}), \quad \forall\, \mathbf{v} \in V \tag{2.20}$$

where $\mathcal{A}(\cdot,\cdot) : V \times V \to \mathbb{R}$ is called bilinear operator and $\mathcal{F}(\cdot) : V \to \mathbb{R}$ is linear operator. In addition, the bilinear operator $\mathcal{A}(\cdot,\cdot)$ has the following two properties, namely:

Continuity

$$\exists\, M > 0 \ \text{ such that } \ \forall\, \mathbf{v}_1, \mathbf{v}_2 \in V, \quad |\mathcal{A}(\mathbf{v}_1,\mathbf{v}_2)| \leq M \|\mathbf{v}_1\|_1 \|\mathbf{v}_2\|_1 \tag{2.21}$$

Ellipticity

$$\exists\, \alpha > 0 \ \text{ such that } \ \forall\, \mathbf{v} \in V, \quad \mathcal{A}(\mathbf{v},\mathbf{v}) \geq \alpha \|\mathbf{v}\|_1^2 \tag{2.22}$$

where $\|\cdot\|_1$ stands for the 1-Sobolev norm, $M, \alpha \in \mathbb{R}$ are constants independent of $\mathbf{v}$; thus, depending only on the specific elasticity problem being considered, and specially the material properties and length scales. Furthermore, by letting $\mathbf{v}_1 = \mathbf{v}_2 = \mathbf{v}$ and combining Eqs. (2.19) to (2.22) results into:

$$c_1\|\mathbf{v}\|_1 \ \leq \ \|\mathbf{v}\|_E \ \leq \ c_2\|\mathbf{v}\|_1 \qquad c_1, c_2 \in \mathbb{R} \qquad \forall \mathbf{v} \in V_h \tag{2.23}$$

which leads to the following remarks:

$L^2(\Omega)$, we could have referred to the Hilbert space $H^1(\Omega)$. Additionally, since we require that $v_i|_\Gamma = 0$ we can refer to $H_0^1(\Omega)$. Clearly, $H_0^1(\Omega) \subset H^1(\Omega)$. Therefore, we could alternatively have written $V = \{\mathbf{v} \mid \mathbf{v} \in [H_0^1(\Omega)]^3\}$. See [17, 18].

Remark 1: The energy norm (2.19) defined in V is equivalent to the 1-Sobolev norm, which means that our "energy space" V inherits all properties of the Sobolev space $H^1(\Omega)$; Furthermore, it states that the range of $\mathcal{A}(\mathbf{u}, \mathbf{v})$ is bounded from below by (2.22) and above by (2.21).

Remark 2: Provided $\mathcal{A}(\mathbf{u}, \mathbf{v})$ represents a "well posed" problem, it is assured $\mathbf{u}$ is unique and corresponds to finite strain energy;

Remark 3: By a well posed problem we mean: (*i.*) the structure is properly supported, hence no rigid body displacements must be possible; (*ii.*) the boundary is sufficiently regular such that the applied surface loads are well defined, i.e., $\mathbf{f}^S \in L^2(\Omega)$.

Consider now the finite element interpolation. We denote by V^h the vector space spanned by all finite element interpolation functions of a particular discretization scheme (h = typical the element size). In other words, V^h is a *finite dimensional* subspace of V. Clearly, $V^h \subset V$, and $\mathbf{v}^h, \mathbf{u}^h \in V^h$, where $\mathbf{v}^h$ is a typical element of V^h and $\mathbf{u}^h$ the finite element solution we are after. Therefore, the finite element problem statement corresponding to (2.20) reads:

$$\text{Find} \quad \mathbf{u}^h \in V^h \quad \text{such that} \quad \mathcal{A}(\mathbf{u}^h, \mathbf{v}^h) = \mathcal{F}(\mathbf{v}^h), \quad \forall\, \mathbf{v}^h \in V^h \tag{2.24}$$

with V^h defined as:

$$V^h = \left\{ \mathbf{v}^h \mid (v_i^h, v_{i,j}^h) \in L^2(\Omega);\ \ v_i^h|_{\Gamma_u} = 0;\ i, j = 1, 2, 3 \right\} \tag{2.25}$$

Endowed with Eqs. (2.15) to (2.22), which correspond to the continuous case, the following properties of the displacement-based finite element interpolation hold:

Property 1

$$\mathcal{A}(\mathbf{e}^h, \mathbf{v}^h) = 0 \qquad \forall\, \mathbf{v}^h \in V^h \tag{2.26}$$

Let $\mathbf{e}^h = \mathbf{u} - \mathbf{u}^h$ be the error between the continuous and discrete solutions of (2.20). Recall that V^h is a normed linear vector space. Therefore, the *vectors*

$\mathbf{e}^h$ and $\mathbf{v}^h$ can be regarded as being "$\mathcal{A}$" orthogonal. Since $\mathbf{u}$ is unique, it follows from (2.22) that, among all $\mathbf{v}^h \in V^h$, $\mathbf{u}^h$ is that particular set of "admissible" functions rendering the minimum strain energy corresponding to $\mathbf{u} - \mathbf{u}^h$.

Property 2

$$\mathcal{A}(\mathbf{u}^h, \mathbf{u}^h) \leq \mathcal{A}(\mathbf{u}, \mathbf{u}) \tag{2.27}$$

From property 1, it follows that

$$\mathcal{A}(\mathbf{u}, \mathbf{u}) = \mathcal{A}(\mathbf{u}^h, \mathbf{u}^h) + \mathcal{A}(\mathbf{e}^h, \mathbf{e}^h)$$

Recall the ellipticity condition $\mathcal{A}(\mathbf{v}, \mathbf{v}) > 0 \quad \forall \mathbf{v} \neq \mathbf{0}$. Therefore, $\mathcal{A}(\mathbf{e}^h, \mathbf{e}^h) \to 0$ iff $\|\mathbf{e}^h\|_E \to 0$, which implies

$$\|\mathbf{u} - \mathbf{u}^h\|_1 \to 0 \quad \text{as} \quad h \to 0$$

In words, as V^h is made continuously closer to V, the error in strain energy becomes smaller, and the finite element solution $\mathbf{u}^h$ converges from below to the strain energy corresponding to the exact solution $\mathbf{u}$.[5]

Property 3

$$\mathcal{A}(\mathbf{e}^h, \mathbf{e}^h) \leq \mathcal{A}(\mathbf{u} - \mathbf{v}^h, \mathbf{u} - \mathbf{v}^h) \qquad \forall \mathbf{v}^h \in V^h \tag{2.28}$$

Using (2.19), we can regard $\|\mathbf{u} - \mathbf{v}^h\|_E^2$ as the "distance" between members of the finite dimensional space V^h and V in which the solution $\mathbf{u}$ lies.

Convergence This equation assures convergence in the energy norm. Following properties (2.26) to (2.28) and by using the continuity (2.21) and ellipticity (2.22) conditions, it can be shown that the finite element solution of our general elasticity problem converges monotonically to the exact solution $\mathbf{u}$ with the error given by Cea's lemma:

$$\|\mathbf{u} - \mathbf{u}^h\|_1 \leq c \; d(\mathbf{u}, V^h) \tag{2.29}$$

[5]Note that, $\|\mathbf{u} - \mathbf{u}^h\|_1 \to 0$ does not necessarily mean that $\mathbf{u}^h \to \mathbf{u}$. Actually, it says that $\mathbf{u} - \mathbf{u}^h$ and their first general derivatives have *measure zero* in $L^2(\Omega)$.

where $c = \sqrt{M/\alpha}$ and $d(\mathbf{u}, V^h) = \inf_{\mathbf{v}^h \in V^h} \|\mathbf{u} - \mathbf{v}^h\|_1$ can be regarded as a measure of the "distance" between the vectors $\mathbf{u}$ and $\mathbf{u}^h$[1]. In other words, provided that the succeeding subspace $V^{2h} \in V$ and contains its predecessor such that $\{V^h \subset V^{2h} \subset \cdots \subset V\}$, it can be demonstrated that the rate of convergence is given by

$$\|\mathbf{u} - \mathbf{u}^h\|_1 \leq \hat{c} h^k \tag{2.30}$$

where the constant $\hat{c} > 0$ is independent of V, k the order of the complete polynomials used and h a typical parameter related to the element size.

2.5 Mixed Interpolation

The displacement-based finite element method has been successfully used in engineering practice. There are, however, two particular problem-areas, namely, plate/shell and near incompressible media analysis, in which the displacement-based finite element is not effective, exhibiting a too stiff response characterized in the literature as *locking* [1].

Shear locking occurs due to the inability of the discrete numerical model to properly represent a zero shear strain state for pure bending problems. *Membrane locking* appears when artificial membrane strains are generated. These phenomena typically occur in beam and thin plate/shell analysis when the thickness t of the element approaches zero. In near incompressible media analysis *volumetric locking* occurs due to the fact that the discrete numerical model does not have a sufficiently rich displacement field satisfying zero volumetric strain constraint ($\epsilon_v = \nabla \cdot \mathbf{u}$) as the Poisson's ratio ν approaches the limit 1/2.

To overcome such (numerical) difficulties, various techniques have been proposed. The main idea is to interpolate the strain and stress fields in addition to the displacement field, giving rise to the so called *mixed* methods.

The common basis of all mixed methods proposed in the literature is the general functional of Hu-Washizu [1], in which displacements, stresses and strains are used as

independent variables (*mixed* fields). The finite element interpolations of these fields can be chosen independently of each other. From the Hu-Washizu functional we can derive the Hellinger-Reissner (H-R) functional (Π_{HR}), in which case the displacements and stresses are the variables.

2.6 Variational Formulation

An alternative approach to obtain the equilibrium governing equations of our elasticity problem is followed by using the calculus of variations. In words, it can be summarized as follows: given a functional $\Pi(\boldsymbol{\phi})$ (a function Π of the functions $\phi_1, \ldots, \phi_n$) find a particular set $\boldsymbol{\phi}^h = \{\phi_1^h, \ldots, \phi_n^h\}$ which makes the functional Π stationary [19]. In other words, for any arbitrary "variation" δ in the functions ϕ_i, denoted $\delta\phi_i$, the corresponding variation $\delta\Pi$ in the functional is zero

$$\delta\Pi = \frac{\partial \Pi}{\partial \phi_1}\,\delta\phi_1 + \cdots + \frac{\partial \Pi}{\partial \phi_n}\,\delta\phi_n = 0 \quad \forall \phi_i \in \boldsymbol{\Phi} \quad i = 1, \ldots, n$$

Since the variations $\delta\phi_i$ are arbitrary, each $\dfrac{\partial \Pi}{\partial \phi_i}$ must vanish.

In our case, the principle of minimum potential energy is the equivalent "variational" statement of our elasticity problem. Let $\Pi(\mathbf{u})$ denote the total potential

$$\Pi(\mathbf{u}) = \tfrac{1}{2}\int_\Omega \boldsymbol{\epsilon}^T \boldsymbol{\tau}\, d\Omega - \int_\Omega \mathbf{u}^T \mathbf{f}^B\, d\Omega - \int_{\Gamma_f} \mathbf{u}^{\Gamma_f^T} \mathbf{f}^S\, d\Gamma \tag{2.31}$$

subjected to

$$\boldsymbol{\tau} = \mathbf{C}\boldsymbol{\epsilon} \tag{2.32}$$

$$\boldsymbol{\epsilon} = \boldsymbol{\partial}_\epsilon \mathbf{u} \tag{2.33}$$

$$\mathbf{u}|_{\Gamma_u} = \mathbf{u}_p \tag{2.34}$$

In the case of linear analysis, the displacement field $\mathbf{u}$ is the independent variable. After introducing (2.32) to (2.34) into (2.31), we invoke stationarity of Π and obtain:

$$\delta\Pi = \delta\left\{\tfrac{1}{2}\int_\Omega \boldsymbol{\epsilon}^T \mathbf{C}\boldsymbol{\epsilon}\, d\Omega - \int_\Omega \mathbf{u}^T \mathbf{f}^B\, d\Omega - \int_{\Gamma_f} \mathbf{u}^{\Gamma_f^T} \mathbf{f}^S\, d\Gamma\right\} = 0$$

This results into:

$$\delta\Pi = \int_\Omega \delta\boldsymbol{\epsilon}^T \mathbf{C}\boldsymbol{\epsilon}\, d\Omega - \int_\Omega \delta\mathbf{u}^T \mathbf{f}^B\, d\Omega - \int_{\Gamma_f} \delta\mathbf{u}^{\Gamma_f^T} \mathbf{f}^S\, d\Gamma = 0 \tag{2.35}$$

which is equivalent to the principle of virtual work (2.7) when we regard the variations $\delta\mathbf{u}$ and $\delta\boldsymbol{\epsilon}$, respectively, as the virtual displacements $\overline{\mathbf{u}}$ and corresponding virtual strains $\overline{\boldsymbol{\epsilon}}$. Note that conditions (2.33) and (2.34) can be regarded as "constraints" which can be incorporated into (2.31) via Lagrange multipliers, in the form

$$\tilde{\Pi} = \Pi - \int_\Omega \boldsymbol{\lambda}_\epsilon^T (\boldsymbol{\epsilon} - \boldsymbol{\partial}_\epsilon \mathbf{u})\, d\Omega - \int_{\Gamma_u} \boldsymbol{\lambda}_u^T \left(\mathbf{u}^{\Gamma_u} - \mathbf{u}_p\right)\, d\Gamma$$

It can be demonstrated that by invoking stationarity of $\tilde{\Pi}$ considering $\mathbf{u}$, $\boldsymbol{\epsilon}$, $\boldsymbol{\lambda}_\epsilon$ and $\boldsymbol{\lambda}_u$ as independent variables, $\boldsymbol{\lambda}_\epsilon$ corresponds to the stresses $\boldsymbol{\tau}$ and $\boldsymbol{\lambda}_u$ corresponds to the surface tractions $\mathbf{f}^{\Gamma_u}$ on Ω_u, resulting into the celebrated Hu-Washizu functional $\Pi_{\text{HW}}(\mathbf{u}, \boldsymbol{\epsilon}, \boldsymbol{\tau}, \mathbf{f}^{\Gamma_u})$ [1]:

$$\begin{aligned} \Pi_{\text{HW}} = {} & \tfrac{1}{2} \int_\Omega \boldsymbol{\epsilon}^T \mathbf{C}\boldsymbol{\epsilon}\, d\Omega - \int_\Omega \boldsymbol{\tau}^T (\boldsymbol{\epsilon} - \boldsymbol{\partial}_\epsilon \mathbf{u})\, d\Omega \\ & - \int_\Omega \mathbf{u}^T \mathbf{f}^B\, d\Omega - \int_{\Gamma_f} \mathbf{u}^{\Gamma_f^T} \mathbf{f}^S\, d\Gamma - \int_{\Gamma_u} (\mathbf{u}^{\Gamma_u} - \mathbf{u}_p)^T \mathbf{f}^{\Gamma_u}\, d\Gamma \end{aligned} \tag{2.36}$$

The flexibility and generality of the Hu-Washizu functional gives more latitude in formulating a variety of finite element discretizations, of which a few are described in the next chapter.

Chapter 3

Some Mixed Interpolation Procedures

Our goal in writing this chapter is to summarize some mixed interpolation procedures published in the literature. We start by recalling the displacement-based finite element formulation derived from the Hu-Washizu functional. Using this framework we then describe the method of incompatible modes, enhanced assumed strain, displacement-pressure interpolation and mixed interpolation of tensorial components. We conclude the presentation by mentioning general conditions to assure stability and convergence of mixed interpolation procedures.

3.1 Introduction

We recall that in the finite element method the volume of the body or domain Ω is partitioned into subdomains Ω_e or finite elements in the form

$$\Omega \approxeq \Omega^h = \bigcup_{e=1}^{ne} \Omega_e$$

Provided each Ω_e is a proper subset of Ω^h we can use the fact that

$$\int_{\Omega^h} (\cdot)\, d\Omega = \int_{\Omega_1} (\cdot)_1\, d\Omega_1 + \cdots + \int_{\Omega_{ne}} (\cdot)_{ne}\, d\Omega_{ne}$$

to write the Hu-Washizu functional (2.31) as

$$\Pi|_{\Omega} = \sum_{e=1}^{ne} \Pi|_{\Omega_e}$$

For each element Ω_e we have

$$\begin{aligned} \Pi_e = & \tfrac{1}{2} \int_{\Omega_e} \boldsymbol{\epsilon}^T \mathbf{C} \boldsymbol{\epsilon} \, d\Omega - \int_{\Omega_e} \boldsymbol{\tau}^T (\boldsymbol{\epsilon} - \boldsymbol{\partial}_\epsilon \mathbf{u}) \, d\Omega \\ & - \int_{\Omega_e} \mathbf{u}^T \mathbf{f}^B \, d\Omega - \int_{\Gamma_{fe}} \mathbf{u}^{\Gamma_f^T} \mathbf{f}^S \, d\Gamma - \int_{\Gamma_{ue}} (\mathbf{u}^{\Gamma_u} - \mathbf{u}_p)^T \mathbf{f}^{\Gamma_u} \, d\Gamma \end{aligned} \tag{3.1}$$

Assuming linear conditions, the displacement field $\mathbf{u}$ is the independent variable and we substitute $\boldsymbol{\epsilon} = \boldsymbol{\partial}_\epsilon \mathbf{u}$ and $\boldsymbol{\tau} = \mathbf{C}\boldsymbol{\epsilon}$ into Π_e (3.1) to obtain:

$$\Pi_e = \tfrac{1}{2} \int_{\Omega_e} \boldsymbol{\epsilon}^T \mathbf{C} \boldsymbol{\epsilon} \, d\Omega - \int_{\Omega_e} \mathbf{u}^T \mathbf{f}^B \, d\Omega - \int_{\Gamma_{fe}} \mathbf{u}^{\Gamma_f^T} \mathbf{f}^S \, d\Gamma$$

where we used the fact that $\mathbf{u} = \mathbf{u}_p$ on Γ_u. Invoking stationarity of Π with respect to $\mathbf{u}$ results

$$\int_{\Omega_e} \delta\boldsymbol{\epsilon}^T \, \mathbf{C} \, \boldsymbol{\epsilon} \, d\Omega = \mathcal{F}(\delta \mathbf{u}) \tag{3.2}$$

with $\boldsymbol{\epsilon}$ being determined from $\mathbf{u}$. Assuming

$$\mathbf{u} = \mathbf{H}\hat{\mathbf{u}} \qquad \boldsymbol{\epsilon} = \mathbf{B}\hat{\mathbf{u}} \tag{3.3}$$

where $\hat{\mathbf{u}}$ is the nodal displacements vector, the corresponding finite element equations are thus

$$\mathbf{K}_e \hat{\mathbf{u}} = \mathbf{R}_e \tag{3.4}$$

where

$$\mathbf{K}_e = \int_{\Omega_e} \mathbf{B}^T \, \mathbf{C} \, \mathbf{B} \, d\Omega \tag{3.5}$$

$$\mathbf{R}_e = \int_{\Omega_e} \mathbf{H}^T \mathbf{f}^B \, d\Omega + \int_{\Gamma_{fe}} \mathbf{H}^{\Gamma_f^T} \mathbf{f}^S \, d\Gamma \tag{3.6}$$

3.2 Incompatible Modes

Recognizing that the classical 4-node isoparametric element (Q1) yields a shear response under pure bending, Wilson *et al* [4] proposed the use of *incompatible displacement* modes $\tilde{\mathbf{u}}$ of quadratic distribution in addition to the usual isoparametric displacement interpolation functions in the form

$$\tilde{\mathbf{u}} = \psi_k \boldsymbol{\delta} \boldsymbol{\alpha}_k \qquad k = 1, 2, 3 \tag{3.7}$$

where $\boldsymbol{\delta}$ is the unit second order tensor, and the vector $\boldsymbol{\alpha}_k^T = \{\alpha_1, \alpha_2, \alpha_3\}_k$ contains typical incompatible mode parameters or generalized incompatible displacements corresponding to the incompatible function $\psi_k(\boldsymbol{\xi}) = 1 - \xi_k^2$, and $\boldsymbol{\xi} = \{\xi_1, \xi_2, \xi_3\}$ are the isoparametric coordinates of a typical element Ω_e. With this assumption we can write the displacement and strain vectors in the following form:

$$\mathbf{u} = \mathbf{H}\hat{\mathbf{u}} + \boldsymbol{\Psi}\boldsymbol{\alpha} \qquad \boldsymbol{\epsilon} = \mathbf{B}_u\hat{\mathbf{u}} + \mathbf{B}_\alpha\boldsymbol{\alpha} \tag{3.8}$$

where $\mathbf{B}_u = \boldsymbol{\partial}_\epsilon \mathbf{H}$ is the discrete differential operator corresponding to the compatible displacements $\mathbf{u}$ and similarly $\mathbf{B}_\alpha = \boldsymbol{\partial}_\epsilon \boldsymbol{\Psi}$ corresponds to the strains associated with $\boldsymbol{\alpha}$. By using the following matrix partitioning

$$\mathbf{u} = \left[\begin{array}{c:c} \mathbf{H} & \boldsymbol{\Psi} \end{array}\right] \left[\begin{array}{c} \hat{\mathbf{u}} \\ \hdashline \boldsymbol{\alpha} \end{array}\right] \qquad \boldsymbol{\epsilon} = \left[\begin{array}{c:c} \mathbf{B}_u & \mathbf{B}_\alpha \end{array}\right] \left[\begin{array}{c} \hat{\mathbf{u}} \\ \hdashline \boldsymbol{\alpha} \end{array}\right] \tag{3.9}$$

the finite element equations read:

$$\begin{bmatrix} \mathbf{K}_{uu} & \mathbf{K}_{u\alpha} \\ \mathbf{K}_{\alpha u} & \mathbf{K}_{\alpha\alpha} \end{bmatrix} \begin{bmatrix} \hat{\mathbf{u}} \\ \boldsymbol{\alpha} \end{bmatrix} = \begin{bmatrix} \mathbf{R} \\ \mathbf{0} \end{bmatrix} \tag{3.10}$$

where

$$\mathbf{K}_{uu} = \int_\Omega \mathbf{B}_u^T \mathbf{C} \mathbf{B}_u \, d\Omega \qquad \mathbf{K}_{u\alpha} = \int_\Omega \mathbf{B}_u^T \mathbf{C} \mathbf{B}_\alpha \, d\Omega \tag{3.11}$$

$$\mathbf{K}_{\alpha u} = \mathbf{K}_{u\alpha}^T \qquad \mathbf{K}_{\alpha\alpha} = \int_\Omega \mathbf{B}_\alpha^T \mathbf{C} \mathbf{B}_\alpha \, d\Omega \tag{3.12}$$

and the incompatible modes can be statically condensed out at element level as

$$\mathbf{K}_e = \mathbf{K}_{uu} - \mathbf{K}_{u\alpha}\,\mathbf{K}_{\alpha\alpha}^{-1}\,\mathbf{K}_{u\alpha}^{T} \tag{3.13}$$

with the final stiffness matrix $\mathbf{K}$ being obtained as usual.

However, the so called Q6 element does not satisfy the patch test, limiting its application to meshes of parallelogram-type elements. Further work by Taylor *et al* [5] altered the Q6 formulation by evaluating the derivatives $\psi_{k,i}$ at the centre of the element such that for an arbitrarily distorted element $\mathbf{B}_\alpha$ will always represent a constant strain state, therefore satisfying the patch test.

Remark 1: The use of incompatible modes violates the fundamental requirement of *continuity* of the assumed displacement field within each element and across element boundaries. In such circumstances one-sided asymptotic convergence to the mathematical model is not guaranteed.

Remark 2: For the specific case of displacement-based interpolation procedures employing non-conforming elements, passing the patch test[1] assures that, as the mesh is gradually refined, convergence to the correct solution of the mathematical model is obtained. However, it should also be noted that, even though the element assemblage passes the patch test, the element itself ought to pass the patch test as well. A classical example of the situation depicted here is the 8-node quadrilateral "reduced" integrated (2x2 Gauss quadrature) element, which is claimed to be useful in the analysis of certain problems. It turned out later that, after passing the patch test, the element's spurious energy mode is sometimes activated during certain analyses spoiling the overall solution. Therefore, to avoid this instability behavior, known as *hourglassing*, an additional requirement is the use of full numerical integration.

[1] After elimination of all rigid body displacements, any patch of elements must (*i.*) accurately represent all constant strain states; (*ii.*) display all natural rigid body mode displacements belonging to the mathematical model being considered; (*iii.*) do not contain any spurious energy modes (equivalent to say that the stiffness matrix contains no more zero eigenvalues than those related to the element's rigid body displacements).

Remark 3: Considering the case of mixed-interpolated finite element procedures, passing the patch test is a *necessary* condition to assert the consistency of the formulation, but it is not a *sufficient* condition that guarantees stability of any mixed-interpolated discretization procedure. For any mixed interpolated procedure, the ellipticity (2.22) and the inf-sup conditions are the rigorous mathematical criteria that should be satisfied in order to have a stable mixed-interpolated formulation. See [1, 20].

3.3 Displacement-Pressure Interpolation

As pointed out earlier, when almost incompressible conditions arise in the analysis of solids, for instance, rubber-like materials are employed or inelastic response is considered, the displacement-based finite element shows poor performance, even when higher-order finite elements are used. It is well known that, as the Poisson's ratio approaches $\nu \to 1/2$ the volumetric strain approaches zero ($\epsilon_V \to 0$). In the limit case of total incompressibility we have $\nabla \cdot \mathbf{u} = 0$, which corresponds to look for a solution in a subspace $K \subset V$ whose members satisfy the incompressibility constraint. Considering the standard displacement-based finite element space V^h, this is a difficult constraint to be satisfied. As a result, the space K^h is usually not rich enough. The practical consequence is the so called locking. Being this the case, alternative interpolation procedures need to be used.

Many finite elements have been proposed in the literature which, to a large extent, are formulated based upon reduced selective integration or penalty type procedures. However, elements based on these approaches have been reported to exhibit spurious energy modes in some analysis cases [1]. Therefore, it is advantageous to use mixed interpolation procedures.

The displacement-pressure formulation is a well established mixed interpolation procedure resulting into reliable and accurate results, and is briefly describe next.

Assuming linear conditions and by substituting $\boldsymbol{\tau} = \mathbf{C}\boldsymbol{\epsilon}$ into the Hu-Washizu

functional (2.36) the Hellinger-Reissner functional is obtained:

$$\Pi_{\mathrm{HR}} = -\tfrac{1}{2}\int_{\Omega} \boldsymbol{\epsilon}^T \mathbf{C}\boldsymbol{\epsilon}\, d\Omega + \int_{\Omega} \boldsymbol{\epsilon}^T \mathbf{C}\boldsymbol{\partial}_{\epsilon}\mathbf{u}\, d\Omega - \mathcal{F}(\mathbf{u}) \tag{3.14}$$

where $\mathcal{F}(\mathbf{u})$ is given in (2.16) and we have used the fact that $\mathbf{u}|_{\Gamma_u} = \mathbf{u}_p$. By splitting the strain tensor into its deviatoric $\boldsymbol{\epsilon}_D$ and volumetric (or spherical) ϵ_V parts as given in (3.15)

$$\boldsymbol{\epsilon}_D = \boldsymbol{\epsilon} - \tfrac{1}{3}\epsilon_V \boldsymbol{\delta} \qquad \text{where} \quad \epsilon_V = \mathrm{tr}(\boldsymbol{\epsilon}) \tag{3.15}$$

it can be demonstrated that the following modified Hellinger-Reissner functional holds [1]:

$$\Pi^*_{\mathrm{HR}} = \tfrac{1}{2}\int_{\Omega} \boldsymbol{\epsilon}_D^T \mathbf{C}_D \boldsymbol{\epsilon}_D\, d\Omega + \tfrac{1}{2}\int_{\Omega} \frac{p^2}{\kappa}\, d\Omega - \int_{\Omega} p(\epsilon_V + \frac{p}{\kappa})\, d\Omega - \mathcal{F}(\mathbf{u}) \tag{3.16}$$

where $\mathbf{C}_D$ is the stress-strain matrix corresponding to the deviatoric stress and strain components, p is the pressure and κ is the bulk modulus. Invoking stationarity of Π^*_{HR} with respect to variations of the independent variables $\mathbf{u}$ and p yields:

$$\int_{\Omega} \delta\boldsymbol{\epsilon}_D^T \mathbf{C}_D \boldsymbol{\epsilon}_D\, d\Omega - \int_{\Omega} \delta\epsilon_V p\, d\Omega = \mathcal{F}(\delta\mathbf{u}) \tag{3.17}$$

$$\int_{\Omega} \delta p(\epsilon_V + \frac{p}{\kappa})\, d\Omega = 0 \tag{3.18}$$

with $\boldsymbol{\epsilon}_D$ and ϵ_V being determined from $\mathbf{u}$. Assuming

$$\mathbf{u} = \mathbf{H}\hat{\mathbf{u}} \qquad\qquad \boldsymbol{\epsilon}_D = \mathbf{B}_D\hat{\mathbf{u}} \tag{3.19}$$

$$p = \mathbf{H}_p\hat{\mathbf{p}} \qquad\qquad \epsilon_V = \mathbf{B}_V\hat{\mathbf{u}} \tag{3.20}$$

the corresponding finite element equations are thus

$$\begin{bmatrix} \mathbf{K}_{uu} & \mathbf{K}_{up} \\ \mathbf{K}_{pu} & \mathbf{K}_{pp} \end{bmatrix} \begin{bmatrix} \hat{\mathbf{u}} \\ \hat{\mathbf{p}} \end{bmatrix} = \begin{bmatrix} \mathbf{R} \\ \mathbf{0} \end{bmatrix} \tag{3.21}$$

where

$$\mathbf{K}_{uu} = \int_{\Omega} \mathbf{B}_D^T \mathbf{C}_D \mathbf{B}_D\, d\Omega \qquad\qquad \mathbf{K}_{up} = \int_{\Omega} \mathbf{B}_V^T \mathbf{H}_p\, d\Omega \tag{3.22}$$

$$\mathbf{K}_{pu} = \mathbf{K}_{up}^T \qquad\qquad \mathbf{K}_{pp} = \int_{\Omega} \mathbf{H}_p^T \frac{1}{\kappa} \mathbf{H}_p\, d\Omega \tag{3.23}$$

To arrive at an effective formulation, the degree of the interpolating polynomials should be judiciously chosen. A reasonable way to proceed is that, for the pressure, the maximum complete interpolating polynomial degree used is $k-1$, where k is the complete polynomial degree used to interpolate the displacement field. On the other hand, the minimum polynomial degree is zero, or a constant pressure. Therefore, the key for obtaining an effective element is to finding the best combination of discrete finite element spaces (displacement and pressure) that, together, result in a locking free element depicting the maximum possible order of convergence.

In the specific case of almost incompressible conditions for solid (and fluid) analysis, both theoretical and numerical studies of the u/p formulation are available in the literature. See [1]. The main findings are that high-order quadrilateral elements $Q_n - P_{n-1}$ and triangular elements $P_n^+ - P_{n-1}$, $n \geq 2$ are effective. However, the 9/4 element was found to lock when $\nu \to 1/2$.

3.4 u/p/e Formulation

In a related approach Pantuso and Bathe [12] have proposed a mixed interpolated 4-node quadrilateral finite element for solid and fluid analysis using the u/p-c formulation[2] which includes a 6-parameter enhanced strain field. The element does not lock when either (almost) incompressible conditions or bending dominated problems are considered. The element passes the patch test and the numerical inf-sup test, and shows very good convergence behavior even for distorted meshes. The originality of this formulation lies in taking advantage of the u/p formulation combined with an enhanced strain field, thus rendering a locking free low-order finite element for general use in solid and fluid linear analysis.

[2]In the u/p formulation the pressure degrees of freedom are internal to each element, thus a discontinuous pressure distribution is obtained, whereas in the u/p-c formulation the pressure is a nodal variable and pressure continuity is imposed.

3.5 Mixed Interpolation of Tensorial Components

In order to develop general and effective locking free finite elements for analysis of plates/shells, Bathe and Dvorkin [6] proposed to interpolate the transverse shear strains in addition to interpolating the transverse displacement and section rotations. A well-chosen interpolated strain field is tied to the interpolated displacement field at certain sampling points; thus, no additional modes are included in the analysis. The successful performance of this formulation coined the concept of Mixed Interpolation of Tensorial Components. The main advantages of interpolating the tensorial shear strain components are: (*i.*) the formulation is very general thus can be extended straightforwardly to general shell elements for linear and nonlinear analysis; (*ii.*) geometric distortion is naturally taken into account; (*iii.*) the interpolation procedure is frame invariant.

In plate analysis when the thickness t becomes smaller, the transverse shear strains γ approach zero and shear locking occurs. This constraint is analogous to the case of almost incompressible analysis, which prompted Bathe and Brezzi [21, 22] to extend the underlying mathematical analysis of the u/p formulation to the case of the MITC plate elements. They have established strong mathematical criteria for the stability and optimality of mixed interpolation procedures.

The shear locking phenomenon has been successfully addressed using the MITC formulation, and in the case of plate analysis convergence studies have been published [1]. However, in the case of general shell analysis the situation is more complex, i.e., depending on geometry and support conditions bending-dominated or membrane-dominated behaviors occur, as pointed out by Chapelle and Bathe [23].

The important point to stress is that an effective shell finite element discretization would give the same rate of convergence whenever a bending-dominated or membrane-dominated behavior is encountered. While a complete mathematical analysis of the existing shell finite elements is not available, a numerical inf-sup test was proposed (Bathe, Iosilevich, Chapelle) [24, 25] and should be used to assess the reliability of new mixed-interpolated shell elements.

3.6 Enhanced Assumed Strains

Simo and Rifai [9] proposed a general framework for formulating mixed assumed strain elements. The strain field is given in the form

$$\boldsymbol{\epsilon} = \boldsymbol{\partial}_\epsilon \mathbf{u} + \tilde{\boldsymbol{\epsilon}} \tag{3.24}$$

with $\tilde{\boldsymbol{\epsilon}}$ the enhanced strain field. In the formulation, the Hu-Washizu variational indicator is modified by using the assumed strain field as given by Eq.(3.24). The resulting 3-field functional has stress, displacement and the "enhanced" assumed strain fields as independent variables. The equivalent discrete variational problem is then derived based upon three basic assumptions which, together, the authors claim assures stability of the formulation. Those conditions are:

- (*i*) The enhanced strain interpolation field and the displacement-interpolated strain field have to be independent of each other. A non mathematical reasoning is that, as the enhanced strain field is being conceived to improve upon the performance of the standard strain field this is a rather natural choice. Mathematically, the violation of this condition leads to a singular system of equations.

- (*ii*) The (independent) stress field is also assumed discontinuous across element boundaries and must contain at least piece-wise constant functions.

- (*iii*) In order to simplify the formulation, the independent enhanced strain field is chosen such that it is L^2-orthogonal to the assumed stress field. As a result, the stress field term drops out from the finite element equations, collapsing the 3-field formulation to a 2-field one.

With these assumptions, the discrete form of Eq. (3.24) is given by

$$\boldsymbol{\epsilon} = \mathbf{B}\hat{\mathbf{u}} + \mathbf{G}\boldsymbol{\alpha} \tag{3.25}$$

where $\mathbf{B} = \boldsymbol{\partial}_\epsilon \mathbf{H}$ is the discrete differential operator corresponding to the displacements $\mathbf{u}$, $\mathbf{G} = \mathbf{T}\mathbf{G}_\xi$ corresponds to the enhanced assumed strain interpolation functions in the physical space, $\mathbf{T}$ is a tensor transformation which maps $\mathbf{G}_\xi$ from the

isoparametric space $\boldsymbol{\xi}$ into the physical space, and $\boldsymbol{\alpha}$ contains the internal element parameters. Specific issues on the stability of the formulation are addressed in [9], but the inf-sup condition was not mentioned.

Within this framework, the elements of Wilson [4] and Taylor [5] can be considered as particular cases.

Andelfinger and Ramm [10] based on Simo and Rifai's [9] work discussed the use of incompatible strains such that all strain fields are complete bilinear (trilinear for 3D analysis) polynomials in the isoparametric space. For a 3D 8-node element, 30 additional incompatible modes are needed, whereas for a 2D 4-node element 7 additional modes are necessary, as shown in Table 3.1. They pointed out that to

u	1	ξ	η	$\xi\eta$					
v					1	ξ	η	$\xi\eta$	incompatible strain modes
$\frac{\partial u}{\partial \xi}$	1		η						ξ $\quad$ $\xi\eta$
$\frac{\partial v}{\partial \eta}$					1	ξ			η $\quad$ $\xi\eta$
$\frac{\partial u}{\partial \eta} + \frac{\partial v}{\partial \xi}$		1	ξ		1		η		ξ η $\quad$ $\xi\eta$

Table 3.1: Polynomial expansion of compatible strains in the 2D isoparametric space.

obtain a volumetric-locking free 3D 8-node element (EAS30) one should add at least 9 incompatible-type modes in order to have the same linear polynomial field for all normal strain components. They also have shown that by using "Wilson's bubble functions" [4], the element is not volumetric-locking free for certain distorted meshes, since the enhanced strain space spanned by those functions does not contain all necessary 9 incompatible-type modes as cited above (which are analogous to the modes shown in Table 3.1 for the 2D case).

Korelc and Wriggers [11] have proposed a modified enhanced strain methodology which employs Taylor expansions of the derivatives of the isoparametric and enhanced shape functions. The assumed strain field is considered of the form:

$$\boldsymbol{\epsilon} = \partial_{\epsilon}\mathbf{u} + \tilde{\boldsymbol{\epsilon}} + \boldsymbol{\epsilon}^{su} \tag{3.26}$$

where the new term ϵ^{su} couples the compatible strain field with the enhanced one. The Hu-Washizu principle is also used. The proposed formulation follows the guidelines set forth by Simo and Rifai [9] and uses the incompatible modes suggested by Taylor *et al* [5]. The resulting enhanced strain matrix is sparse since the incompatible modes are uncoupled. The 3D 8-node element proposed in this formulation (QS/E9) uses only 9 incompatible-type modes, whereas the 3D element proposed by Simo, Armero and Taylor [26] (Q1/E9) uses 9 incompatible-type modes, but was found to lock and to present spurious energy modes when severely distorted when used in the context of geometrically nonlinear analysis. Further work by Simo, Armero and Taylor [27] presented an improved formulation (QM1/E12) of the original element, including 12 incompatible-type modes and employing a special quadrature rule. The 3D 8-node element proposed by Korelc and Wriggers [11] presented good results when used in severely distorted meshes. However, since the QS/E9 element uses Taylor expansions defined in the physical space, this renders the element not frame invariant.

There is no report indicating whether the above mentioned elements satisfy the numerical inf-sup test, whereas the $u/p/e$ element proposed by Pantuso and Bathe [12] passes the numerical inf-sup test in 2D linear analysis. Table 3.3 summarizes the main characteristics of the aforementioned elements.

Andelfinger and Ramm [10] stated that the EAS7 element (and its 3D counterpart, EAS30) is equivalent to the 5β (18β) quadrilateral element due to Pian and Sumihara [2], after inspecting the numerically integrated stiffness matrices of these elements. Later work by Yeo and Lee [28] formally proves the findings of Andelfinger and Ramm and also provides the conditions under which the equivalence of the assumed enhanced strain and the assumed stress methodologies holds.

$$\mathbf{G}_{\xi}^{4} = \begin{bmatrix} \xi & 0 & 0 & 0 \\ 0 & \eta & 0 & 0 \\ 0 & 0 & \xi & \eta \end{bmatrix} \tag{3.27}$$

$$\mathbf{G}_{\xi}^{5} = \begin{bmatrix} \xi & 0 & 0 & 0 & \xi\eta \\ 0 & \eta & 0 & 0 & -\xi\eta \\ 0 & 0 & \xi & \eta & \xi^2 - \eta^2 \end{bmatrix} \tag{3.28}$$

$$\mathbf{G}_{\xi}^{6} = \begin{bmatrix} \xi & 0 & 0 & 0 & \xi\eta & 0 \\ 0 & \eta & 0 & 0 & 0 & \xi\eta \\ 0 & 0 & \xi & \eta & 0 & 0 \end{bmatrix} \tag{3.29}$$

$$\mathbf{G}_{\xi}^{7} = \begin{bmatrix} \xi & 0 & 0 & 0 & \xi\eta & 0 & 0 \\ 0 & \eta & 0 & 0 & 0 & \xi\eta & 0 \\ 0 & 0 & \xi & \eta & 0 & 0 & \xi\eta \end{bmatrix} \tag{3.30}$$

Table 3.2: Basis functions used in some EAS elements for the case of plane stress and plane strain conditions.

	Element	Ref.	Class	Eq.	No. modes	Locking free		Pass inf-sup
						shear	vol.	
2D	QM6	[5]	u/ϵ	(3.27)	4	Y	Y	N/A
	EAS5	[9]	u/ϵ	(3.28)	5	Y	Y	N/A
	EAS7	[10]	u/ϵ	(3.30)	7	Y	Y	N/A
	4/4/6	[12]	$u/p/\epsilon$	(3.29)	6	Y	Y	Y
3D	Q1/E9	[26]	u/ϵ		9	N	N	N/A
	QM1/E12	[27]	u/ϵ		12	Y	Y	N/A
	EAS30	[10]	u/ϵ		30	Y	Y	N/A
	QS/E9	[11]	u/ϵ		9	Y	Y	N/A
	8/8/15	[12]	$u/p/\epsilon$		15	Y	Y	N/A

Table 3.3: Comparison of elements properties.

3.7 Other Procedures

3.7.1 Assumed Stress Methods

From the Hu-Washizu functional we can derive the Hellinger-Reissner (H-R) functional (Π_{HR}), in which the displacements and stresses are the variables. Based on the H-R functional, Pian and Sumihara [2] developed a 4-node quadrilateral element (and corresponding 8-node hexahedra element), which has been reported in the literature to exhibit good convergence. See [3] and references therein. However, in this approach the assumed stresses have to satisfy the equilibrium equations *a priori* making use of inverse constitutive relations. Thus, extension of this development to nonlinear analysis is not straightforward because standard algorithms in nonlinear analysis are based on strain measures with stresses being evaluated *a posteriori.*

3.7.2 Use of Bubbles

The use of "bubble" functions in the form

$$\phi_2 = (1-\xi_1^2)(1-\xi_2^2) \qquad \psi_2 = \zeta_1\zeta_2\zeta_3 \qquad \zeta_1 = 1-\zeta_2-\zeta_3 \tag{3.31}$$

$$\phi_3 = (1-\xi_1^2)(1-\xi_3^2)(1-\xi_3^2) \qquad \psi_3 = \zeta_1\zeta_2\zeta_3\zeta_4 \qquad \zeta_1 = 1-\zeta_2-\zeta_3-\zeta_4 \tag{3.32}$$

$$\xi_i \in [-1,1] \qquad \zeta_i \in [0,1] \qquad \zeta_i = \frac{\Omega_i}{\Omega} \tag{3.33}$$

have an attractive property of vanishing along the element boundaries, thus rendering compatible finite elements for which internal degrees of freedom can be statically condensed out. Here ϕ_i refers to quadrilateral 2D and 3D elements, and ψ_i refers to triangular 2D and 3D elements.

However, when attempting to enrich a finite element subspace by using these functions one can demonstrate that [29], in the case of elliptic problems, there is no advantage, since the internal degrees of freedom do not change the vertex unknowns, unless body forces are present.

Chapter 4

Benchmarking

In this chapter we assess the performance of some quadrilateral elements employed in the analysis of classical problems. The elements considered are labeled as: Q1 which corresponds to the displacement-based element, the PS or 5β-I element of Pian and Sumihara [2], the $u/p/e$ (UPE) element proposed by Pantuso and Bathe [12] and the EASn family of enhanced assumed strain elements. Here, we use the EASn elements, with $n = 4, 5, 6, 7$ denoting the number of enhanced strain parameters such that: EAS4 corresponds to the incompatible element QM6 of Taylor [5], EAS5 is the 5 parameter-element of Simo and Rifai [9], EAS7 corresponds to the element proposed by Andelfinger and Ramm [10]. The author has implemented the EAS elements using the user-supplied option available in ADINA©, which is gratefully acknowledged.

4.1 Cantilever Beam

Consider a cantilever beam subjected to pure bending as depicted in Fig. 4-1. To model this problem plane stress conditions are assumed. The exact solution is obtained by using a mesh of 2 non-distorted assumed stress or assumed strain finite elements. However, this degree of accuracy is not shared by all "enhanced" finite elements when used in distorted meshes. The calculated vertical displacement v of the free tip is compared against the analytical solution as the mesh is gradually distorted by rotating the common edge of the elements. The chart in Fig. 4-2 summarizes these

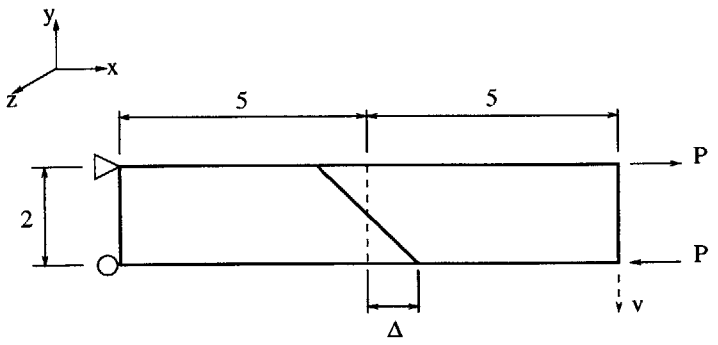

Figure 4-1: Beam bending $E = 1,500$ and $\nu = 0.0$

results.

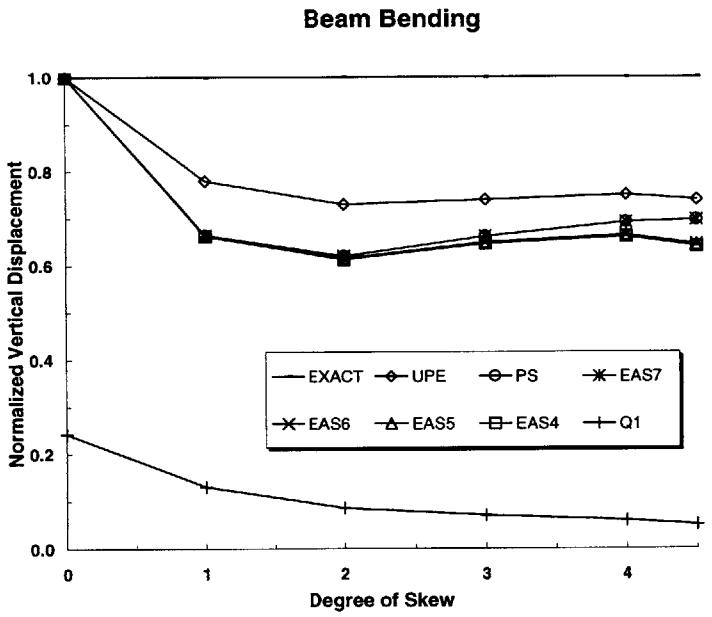

Figure 4-2: Sensitivity to geometric distortion Δ.

As can be seen, the EAS elements have almost the same sensitivity to geometric distortion, with a slight advantage to the EAS7 element. Also note that the EAS7 and PS elements give same results, as pointed out in [10, 28]. The $u/p/e$ element of Pantuso and Bathe [12] seems to be the least sensitive to geometric distortions.

4.2 Cook's Membrane

A tapered beam clamped on its left edge and subjected to an uniformly distributed shearing load F applied on the opposite edge is shown in Fig. 4.2. Plane stress conditions are assumed and quadrilateral elements are used. We consider a sequence of

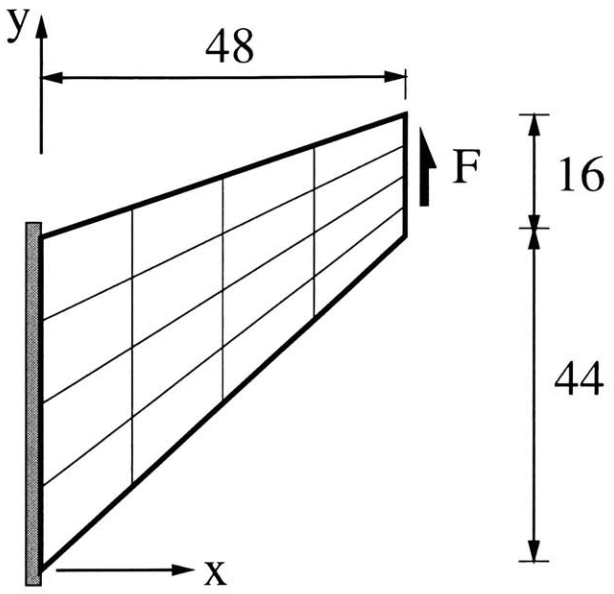

Figure 4-3: Cook's membrane. Plane stress, unit thickness, $E = 1$, $\nu = 1/3$

uniform meshes of $\{2, 4, 8, 16, 32\}$ elements (per side) to calculate the vertical displacement at the mid-side of the free edge. It can be readily seen from Fig. 4.2 that the assumed strain elements depict very good coarse-mesh accuracy as opposed to the displacement-based element. Figure 4.2 shows a smoothed plotting of the τ_{yy} for the case of 32x32 mesh of EAS7 elements.

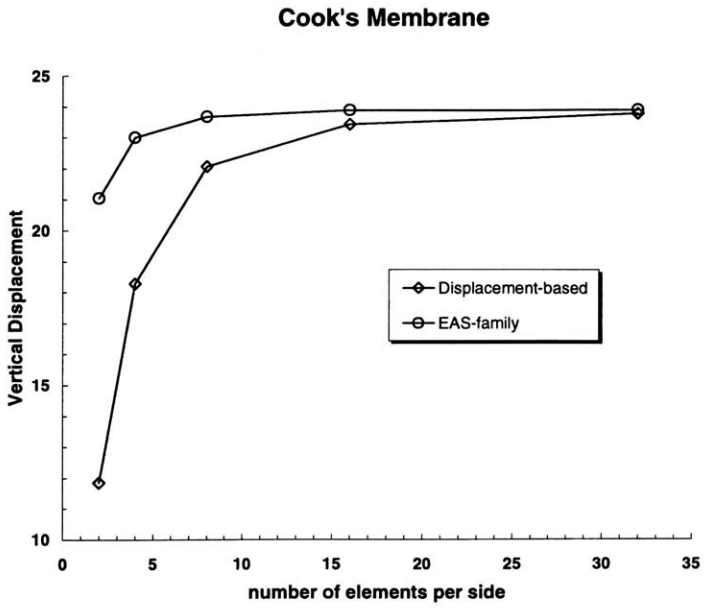

Figure 4-4: Uniform shearing load. Vertical displacement of the mid-point of the free-edge is considered.

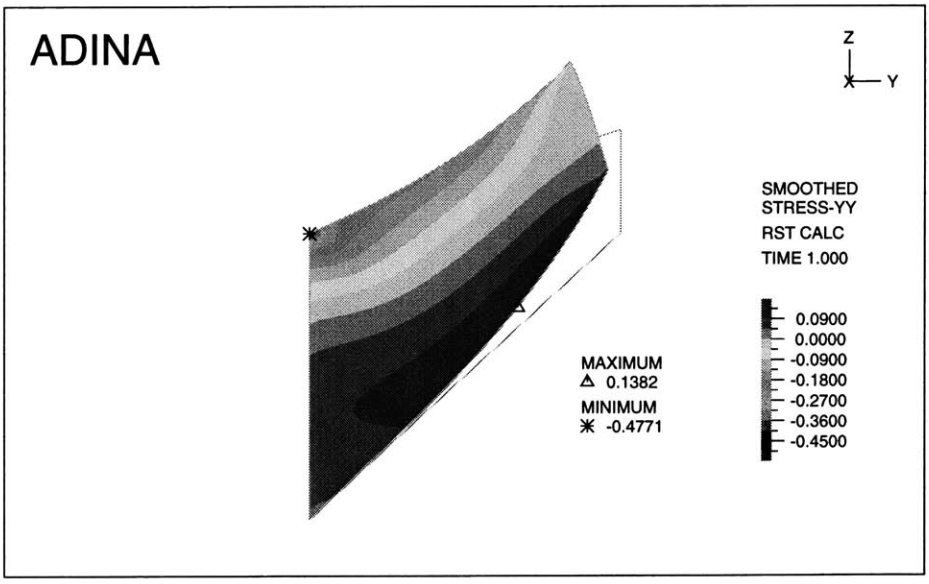

Figure 4-5: Element EAS7: Smoothed τ_{yy}.

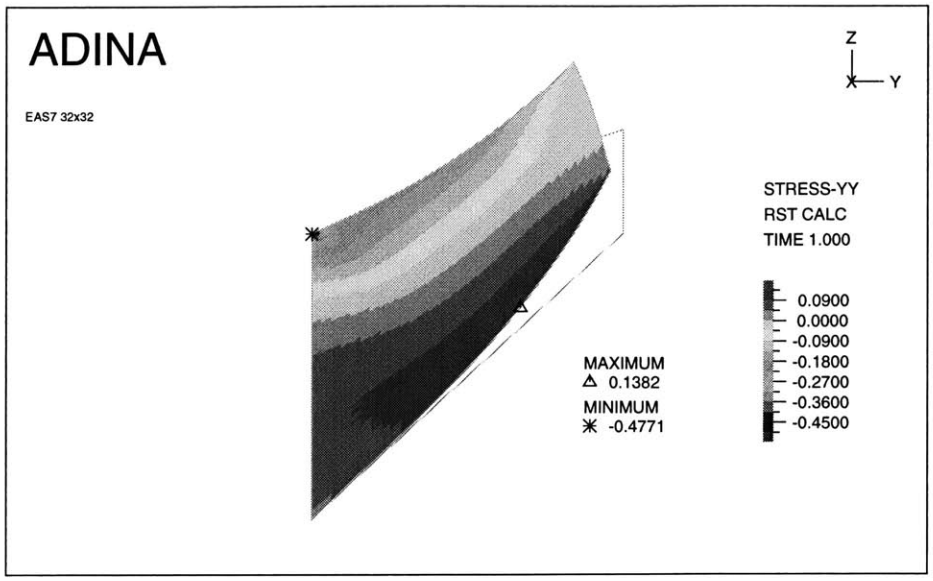

Figure 4-6: Element EAS7: Non-smoothed τ_{yy}.

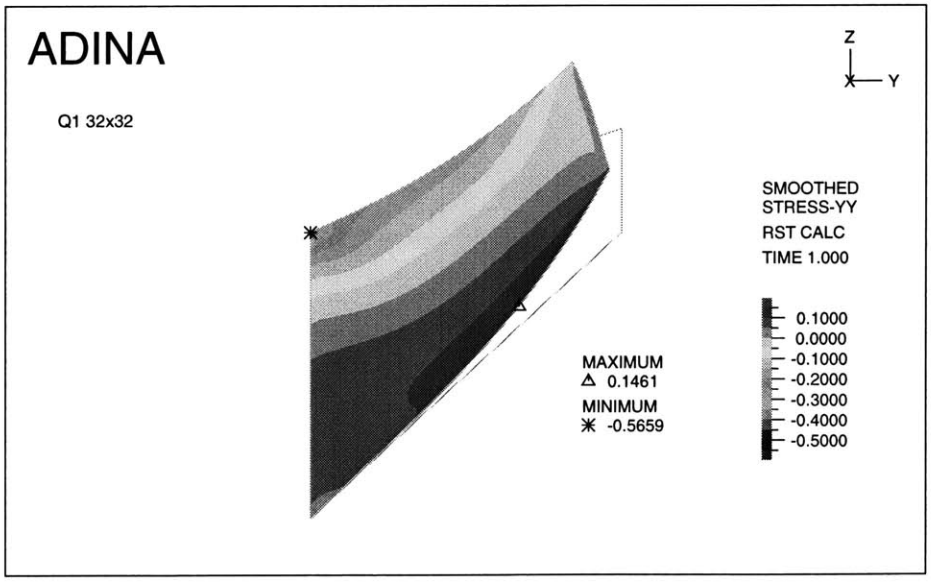

Figure 4-7: Element Q1: Smoothed τ_{yy}.

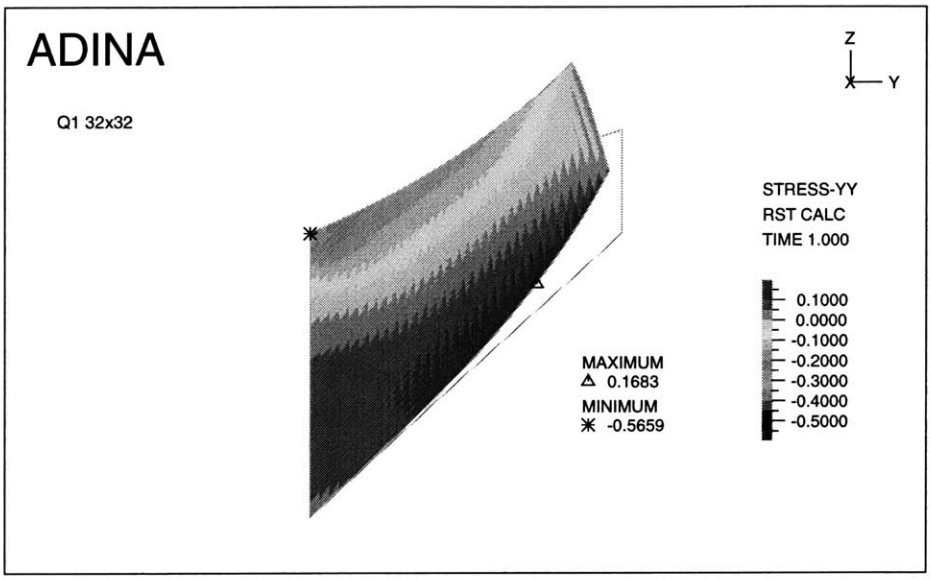

Figure 4-8: Element Q1: Non-smoothed τ_{yy}.

4.3 Driven Cavity

In order to evaluate the performance of the enhanced strain-based elements in almost incompressible elasticity situations, we consider the Stokes flow problem which is governed by the same differential equations as isotropic incompressible elasticity. In the problem solution we take the velocity field $\mathbf{u}$ of the flow problem to correspond to the displacement field, and the dynamic viscosity μ to correspond to the shearing modulus G used in elasticity. The problem considered is to calculate the pressure distribution inside a square cavity which has zero velocities $\mathbf{u}$ (displacements) prescribed at all edges except at the top edge, which has $u = 1$ and $v = 0$, as shown in Fig. 4-9. Plane

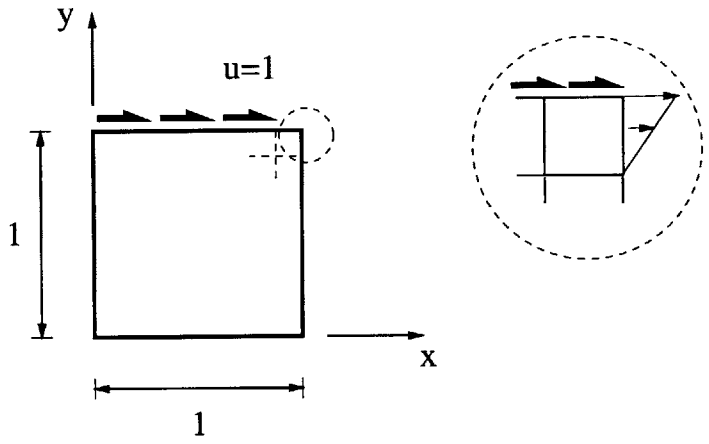

Figure 4-9: Driven cavity. Boundary condition for all edges $u = v = 0$, except top edge where $u = 1, v = 0$.

strain conditions are assumed, and the analysis was carried out by using 10x10 and 20x20 meshes. As expected, the pure displacement-based element spoils the analysis as Poisson's ratio approaches 1/2, whereas the assumed strain elements retain a good accuracy as the mesh is refined. The "velocity" field is shown in Figs. 4-10 and 4-11 for the 10x10 mesh of Q1 and EAS7 elements.

Comparative plots of the pressure results are shown in Figs. 4-12–4-14. Note that pressure values shown are smoothed nodal results evaluated from the stress field.

For the case of the 20x20 mesh, depicted in Figs. 4-15– 4-16, similar results are obtained.

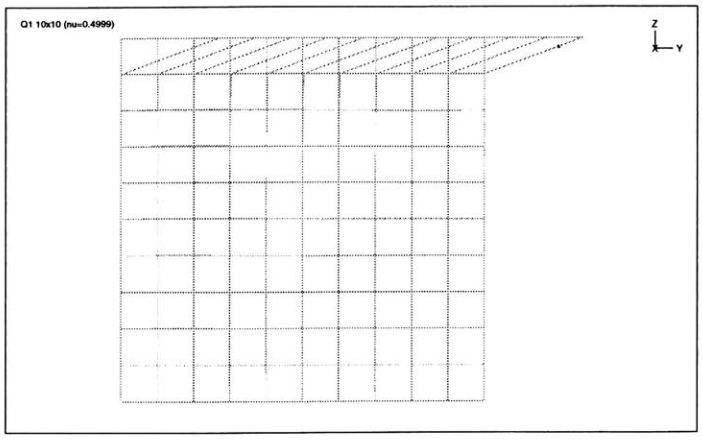

Figure 4-10: Q1 element. Velocity field 10x10 mesh.

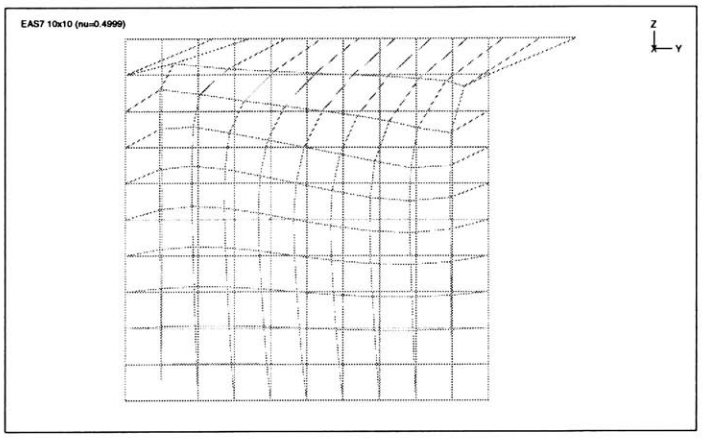

Figure 4-11: EAS7 element. Velocity field 10x10 mesh.

Among the 2D elements we considered, the $u/p/e$ element proposed by Pantuso and Bathe [12] seems to be the least sensitive to geometric distortions. Considering that it uses a 6-parameter assumed strain field, passes the numerical inf-sup test and performs equally well in almost incompressible situations, its general use in linear analysis is recommended.

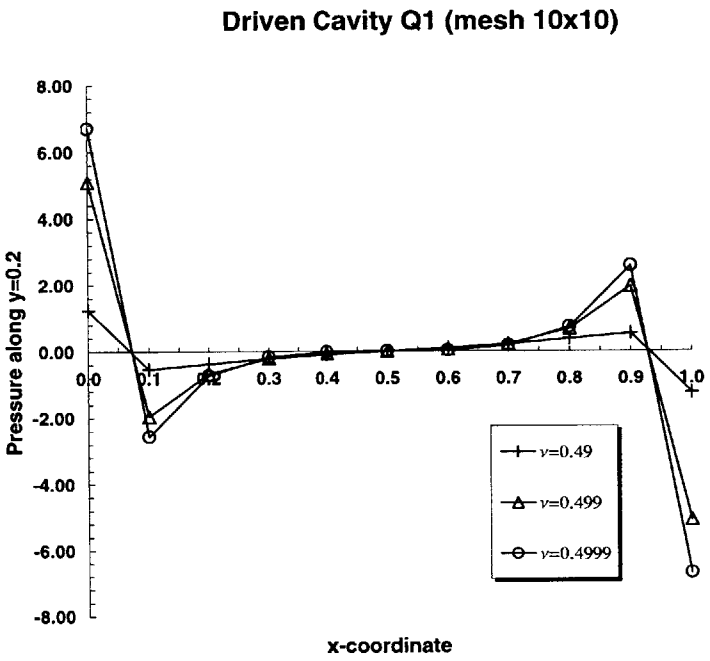

Figure 4-12: Q1 Element: Pressure distribution at $y = 0.2$ mesh 10x10.

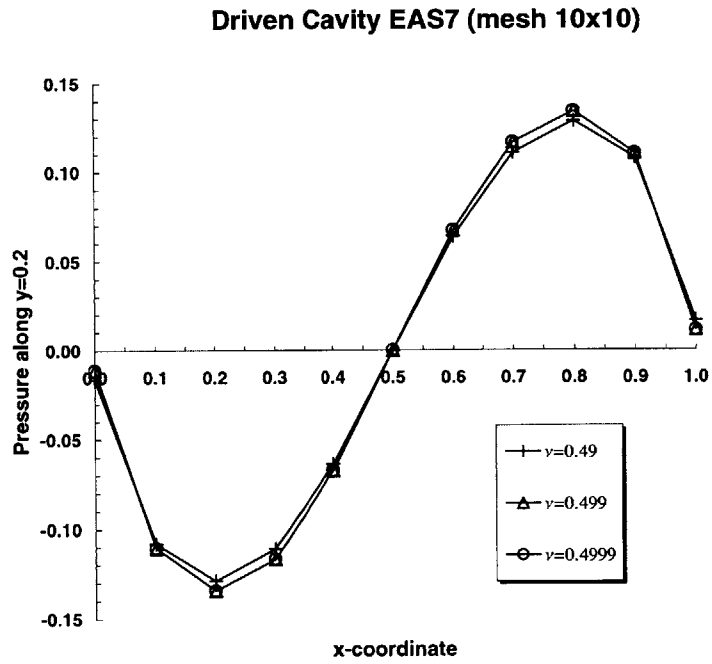

Figure 4-13: EAS7 Element: Pressure distribution at $y = 0.2$ mesh 10x10.

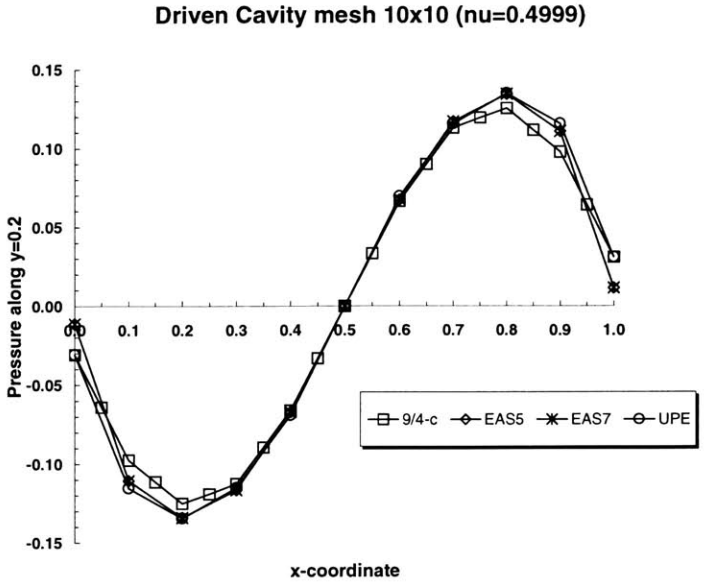

Figure 4-14: Comparison of elements: Pressure distribution at $y = 0.2$ mesh 10x10.

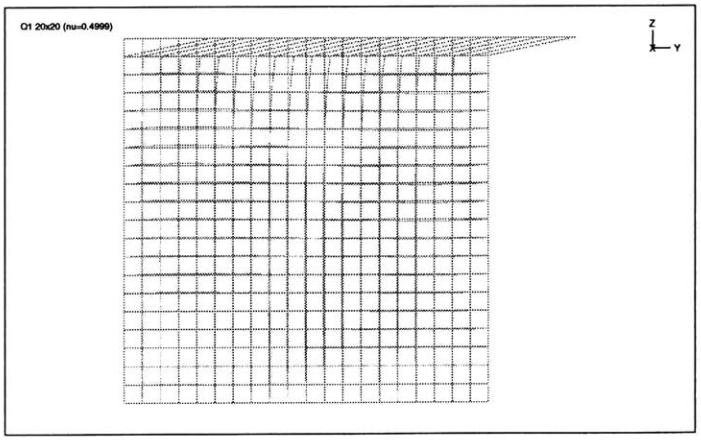

Figure 4-15: Q1 element. Velocity field 20x20 mesh.

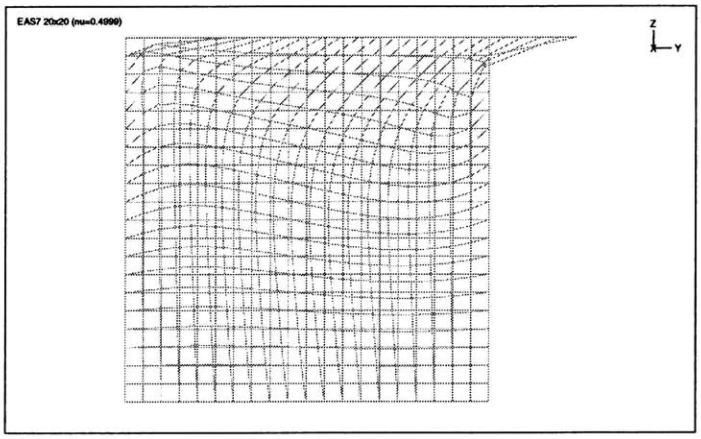

Figure 4-16: EAS7 element. Velocity field 20x20 mesh.

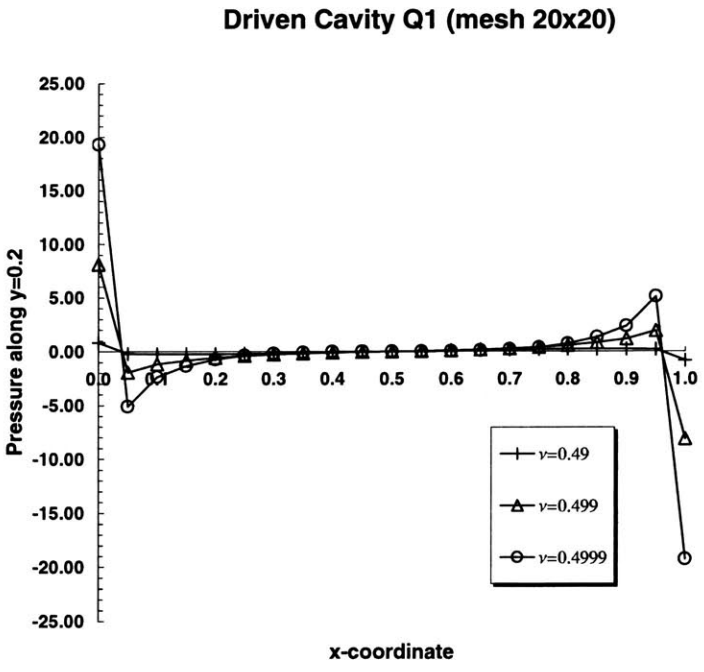

Figure 4-17: Q1 Element: Pressure distribution at $y = 0.2$ mesh 20x20.

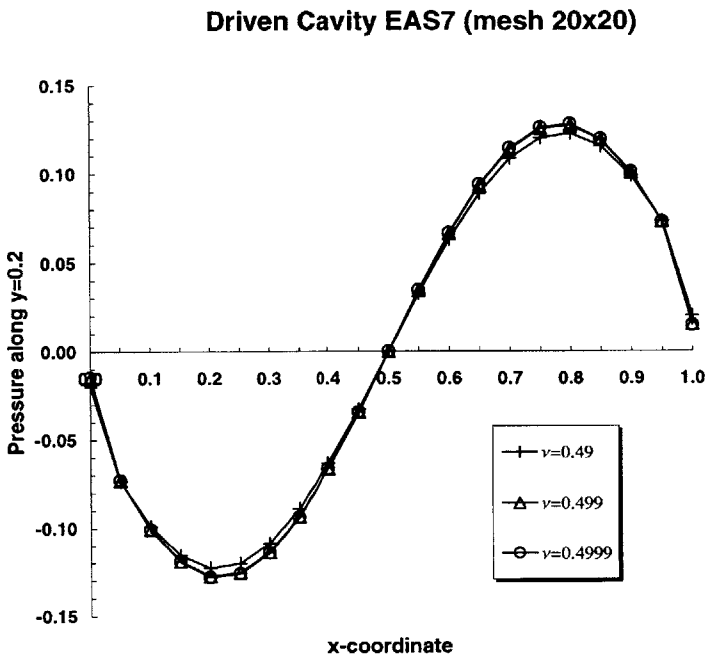

Figure 4-18: EAS7 Element: Pressure distribution at $y = 0.2$ mesh 20x20.

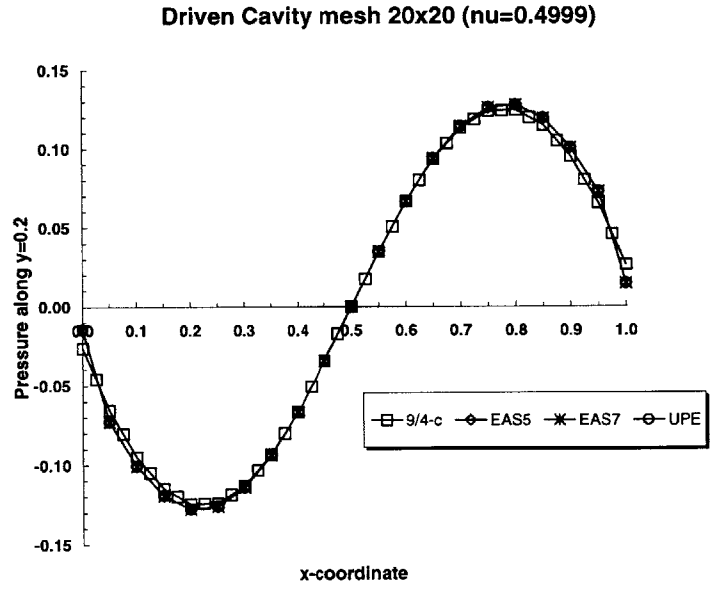

Figure 4-19: Comparison of elements: Pressure distribution at $y = 0.2$ mesh 20x20.

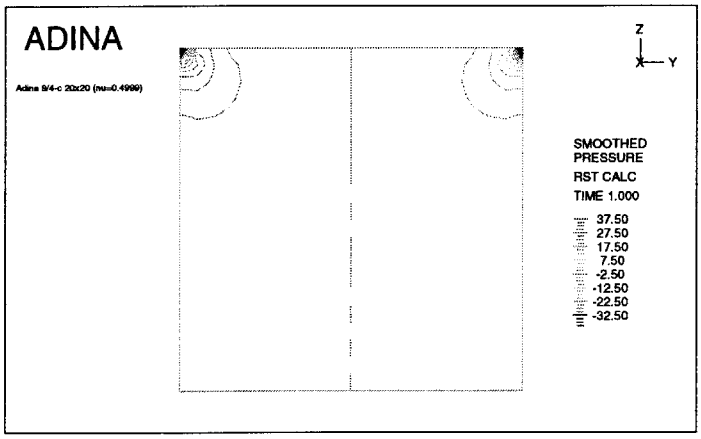

Figure 4-20: 9/4-c Element: Pressure contours mesh 20x20.

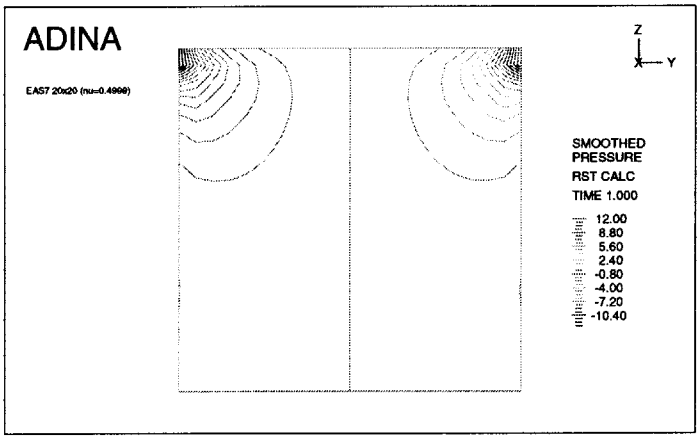

Figure 4-21: EAS7 Element: Pressure contours mesh 20x20.

Chapter 5

Closure

We close this presentation by summarizing some fundamental aspects of using mixed interpolation procedures. First, let us recall our main objective: to identify efficient mixed interpolation procedures proposed in the literature envisioning to develop reliable low-order triangular and tetrahedral elements for solid and fluid analysis.

Based on what we learned in this research, we consider that a reliable finite element, should ideally have the following properties:

- be continuum mechanics based,
- satisfy the patch test,
- be invariant and insensitive to geometric distortions,
- have a minimum of stress/strain parameters,
- provide accurate displacement and stress calculations irrespective of material conditions,
- use full numerical integration,
- use no artificial parameters,
- satisfy the inf-sup condition (locking-free response and no spurious zero energy modes),

- work well in small and large strain conditions,
- have a consistent variational basis.

We noticed a strong trend in using the assumed strain framework as a means for designing improved elements Although many procedures with variational basis have been successfully applied to solve problems, only few of them represent reliable mixed interpolation discretizations. Namely, we note the lack of studying whether the elements satisfy the inf-sup condition. Namely, two conditions should be satisfied: (*i.*) **ellipticity** condition of the bilinear forms associated with the mixed interpolation and (*ii.*) the **inf-sup** condition. The former is usually satisfied if appropriate interpolation functions are used and full numerical integration is employed. Satisfying the ellipticity condition ensures solvability. The inf-sup is a general condition for stability and optmality. It is difficult to evaluate analytically; however, numerical tests have been proposed and should be used. Satisfying the inf-sup condition assures stability and optimality of the mixed-interpolated procedure.

In engineering practice, elements lacking generality and failing to fulfill these basic requirements should be ruled out if a serious engineering analysis is considered.

Bibliography

[1] K. J. Bathe. *Finite Element Procedures.* Prentice-Hall, 1996.

[2] T. H. H. Pian and K. Sumihara. Rational approach for assumed stress finite elements. *International Journal for Numerical Methods in Engineering*, 20:1685–1695, 1984.

[3] T. H. H. Pian. State-of-the-art development of hybrid/mixed finite element method. *Finite Element in Analysis and Design*, 21:5–20, 1995.

[4] E. L. Wilson, R. L. Taylor, W. P. Doherty, and J. Ghaboussi. Incompatible displacement models. In S. J. Fenves *et al*, editor, *Numerical and Computer Methods in Structural Mechanics*, pages 43–, New York, 1973. Academic Press.

[5] R. L. Taylor, P. J. Beresford, and E. L. Wilson. A non-conforming element for stress analysis. *International Journal for Numerical Methods in Engineering*, 10(6):1211–1219, 1976.

[6] K. J. Bathe and E. N. Dvorkin. A formulation of general shell elements – the use of mixed interpolation of tensorial components. *International Journal for Numerical Methods in Engineering*, 22(3):697–722, 1986.

[7] E. N. Dvorkin and S. I. Vasolo. A quadrilateral 2d finite element based on mixed interpolation of tensorial components. *Engineering Computations*, 6:217–224, 1989.

[8] R. A. Radovitzky and E. N. Dvorkin. A 3d element for non-linear analysis of solids. *Communications in Numerical Methods in Engineering*, 10:183–194, 1994.

[9] J. C. Simo and M. S. Rifai. A class of mixed assumed strain methods and the method of incompatible modes. *International Journal for Numerical Methods in Engineering*, 29:1595–1638, 1990.

[10] U. Andelfinger and E. Ramm. EAS-elements for two-dimensional, three-dimensional, plate and shell structures and their equivalence to HR-elements. *International Journal for Numerical Methods in Engineering*, 36:1311–1337, 1993.

[11] J. Korelc and P. Wriggers. An efficient 3d enhanced strain element with Taylor expansion of the shape functions. *Computational Mechanics*, 19:30–40, 1996.

[12] D. Pantuso and K. J. Bathe. A four-node quadrilateral mixed-interpolated element for solids and fluids. *Mathematical Models and Methods in Applied Sciences*, 5(8):1113–1128, 1995.

[13] D. Chapelle and K. J. Bathe. The inf-sup test. *Computers & Structures*, 47(4/5):537–545, 1993.

[14] S. Timoshenko and J. N. Goodier. *Theory of Elasticity.* McGraw-Hill, New York, 3rd edition, 1970.

[15] L. E. Malvern. *Introduction to the Mechanics of a Continuous Medium.* Prentice-Hall, Inc., 1969.

[16] O. C. Zienkiewicz and K. Morgan. *Finite Elements and Approximation.* John Wiley & Sons, 1983.

[17] G. Strang and G. J. Fix. *An Analysis of the Finite Element Method.* Prentice-Hall, Inc., 1973.

[18] J. T. Oden. *Applied Functional Analysis.* Prentice-Hall, Inc., 1979.

[19] K. Washizu. *Variational Methods in Elasticity and Plasticity.* Pergamon Press, 3rd edition, 1982.

[20] F. Brezzi and K.J. Bathe. A discourse on the stability conditions for mixed finite element formulations. *Computer Methods in Applied Mechanics and Engineering*, 82:27–57, 1990.

[21] K.J. Bathe and F. Brezzi. On the convergence of a four-node plate-bending element based on mindlin/reissner plate theory and a mixed interpolation. In J.R. Whiteman, editor, *The Mathematics of Finite Elements and Applications V*, pages 491–503. Academic Press, New York, 1985.

[22] F. Brezzi and K.J. Bathe. The inf-sup condition, equivalent forms and applications. In K.J. Bathe and D.R.J. Owen, editors, *Reliability of Methods for Engineering Analysis*, pages 197–219. Pineridge,Swansea., 1986.

[23] D. Chapelle and K. J. Bathe. Fundamental considerations for the finite element analysis of shell structures. *Computers & Structures*, 66(1):19–36, 1998.

[24] A. Iosilevich, K.J. Bathe, and F. Brezzi. On evaluating the inf-sup condition for plate bending elements. *International Journal for Numerical Methods in Engineering*, 40:3639–3663, 1997.

[25] K. J. Bathe, A. Iosilevich, and D. Chapelle. On evaluating the inf-sup condition for shell elements. *Computers & Structures*, submitted, 1999.

[26] J.C. Simo and F. Armero. Geometrically non-linear enhanced strain mixed methods and the method of incompatible modes. *International Journal for Numerical Methods in Engineering*, 33:1413–1449, 1992.

[27] J. C. Simo, F. Armero, and R. L. Taylor. Improved versions of assumed enhanced strain tri-linear elements for 3d finite deformation problems. *Computational Methods in Applied Mechanics and Engineering*, 110:359–386, 1993.

[28] S.T. Yeo and B.C. Lee. Equivalence between enhanced assumed strain method and assumed stress hybrid method based on the Hellinger-Reissner principle. *International Journal for Numerical Methods in Engineering*, 39:3083–3099, 1996.

[29] L. P. Franca and C. Farhat. On the limitations of bubble functions. *Computer Methods in Applied Mechanics and Engineering*, 117:225–230, 1994.